Soil & Tillage Research 251 (2025) 106532

Contents lists available at ScienceDirect

Soil & Tillage Research

journal homepage: www.elsevier.com/locate/still

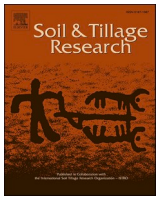

Linking measurable and conceptual phosphorus pools (in APSIM) enables quantitative model initialisation

Yunru Lai [a,i,*], Jonathan J. Ojeda [b,c,i], Simon Clarendon [d,e,i], Nathan Robinson [f,i], Enli Wang [g], Keith G. Pembleton [b,h,i]

[a] Centre for Sustainable Agricultural Systems, University of Southern Queensland, UniSQ Springfield Education City, Sinnathamby Blvd, Springfield Central, QLD 4300, Australia
[b] Centre for Sustainable Agricultural Systems, University of Southern Queensland, West Street, Toowoomba, QLD 4350, Australia
[c] Terradot, Stanford, CA 94305, United States
[d] Department of Primary Industries and Regional Development, 444 Albany Hwy, Albany, WA 6331, Australia
[e] New South Wales Department of Primary Industries, Tamworth Agricultural Institute, Tamworth, NSW 2340, Australia
[f] Centre for eResearch and Digital Innovation, Federation University Australia, Mt Helen, VIC 3350, Australia
[g] CSIRO Agriculture and Food, Cluniess Ross Street, Black Mountain, ACT 2601, Australia
[h] School of Agriculture and Environmental Science, University of Southern Queensland, West Street, Toowoomba, QLD 4350, Australia
[i] Cooperative Research Centre for High Performance Soils, Level 1, IDC Building, University of Newcastle, University Drive, Callaghan, NSW 2308, Australia

ARTICLE INFO

Keywords:
APSIM
P pools
Model initialisation
Model inputs
Crop-soil interactions

ABSTRACT

Phosphorus (P) is an essential plant macro-nutrient, yet it is deficient in 65 % of agricultural soils worldwide. Agricultural systems models enable the integration of plant-soil-climate-management interactions to investigate crop responses to P fertilisation and improve P use efficiency. However, current models cannot align their modellable P pools with values obtained from soil tests. This limits their applicability since soil testing is the most widely used tool to assess soil P status, which is then used to predict fertiliser P requirements based on assumed crop P demand for optimal growth in the field. Our study introduces a modelling framework akin to inversely modelling in the Agricultural Production Systems sIMulator (APSIM) to quantitatively derive the most likely P modelling parameters for different soils and empirically link them to common soil P test values. The methodology was first tested using data from an 8-year alfalfa (syn. lucerne) experiment (1997–2004) on two soil types in the mid-west of the United States to establish the adequacy of the P modelling framework in APSIM. We then extended this approach to eight Australian soil types using a simulation study based on known wheat yield response curves to soil P tests to derive empirical relationships between the labile P values in APSIM and common soil test P values (Bray-2 P and Colwell P) for the soils studied. Cross-validation yielded an average R^2 of 0.98 and an average Lin's Concordance Correlation Coefficient (CCC) of 0.92. Our work thus enables the initialisation of the labile P pool in APSIM using Bray-2 P and Colwell P data, enhancing the usability and accuracy of agricultural systems models in predicting crop P requirements and optimising P fertiliser use across diverse soil types in different agro-climatic regions.

1. Introduction

Phosphorus (P) is essential to life, yet tightly cycled ecologically, with a widespread deficiency in marine, freshwater, and terrestrial ecosystems (Childers et al., 2011). The availability of P limits crop production on more than 65 % of arable soils globally (Cakmak, 2002). The application of P fertilisers is therefore often required to increase the pool of plant-available P due to P uptake by crops and subsequent removal off site (Jiménez et al., 2019). Mineral P supplies are spatially variable, non-renewable, and rapidly depleting (Childers et al., 2011). At the same time, P is an aquatic pollutant with off-site migration risking the health of waterways (Carpenter et al., 1998; Metson et al., 2015). The active management of P cycling is thus considered one of the twenty-first century's greatest global sustainability challenges (Cordell and White, 2014).

Process-based agricultural systems models allow the understanding

* Corresponding author.
E-mail address: Chloe.Lai@unisq.edu.au (Y. Lai).

https://doi.org/10.1016/j.still.2025.106532
Received 22 May 2024; Received in revised form 14 February 2025; Accepted 2 March 2025
Available online 11 March 2025
0167-1987/© 2025 The Author(s). Published by Elsevier B.V. This is an open access article under the CC BY license (http://creativecommons.org/licenses/by/4.0/).

of nutrient cycling and investigation of phenological and physiological crop responses to improve fertiliser use efficiency by integrating genotype × environment × management interactions (Brown et al., 2014). However, research in soil-crop P modelling has received less attention compared to nitrogen (N) and carbon (C) modelling (Das et al., 2019). One major challenge in P modelling is that current agricultural systems models have a limited ability to match laboratory-measured (soil test) P fractions to the conceptual P pools of the models for soils with different mineral properties (Das et al., 2019). Since soil testing is the most widely used tool to predict the P demands for optimal crop growth, this limits the potential of P modelling to improve P efficiency for agricultural production.

The Agricultural Production Systems sIMulator (APSIM; Keating et al., 2003; Holzworth et al., 2014) has been tested for its ability to simulate crop responses to soil solution P fractions through the conceptual labile P pool (*e.g.* Fosu-Mensah et al., 2012; Wang et al., 2014; Ahmed et al., 2018; Raymond et al., 2021), which represents readily available P for crops (Delve et al., 2009). The initialisation of P modelling parameters in such research, however, largely relied on expert knowledge and manual adjustment. The uncertainties with this model initialisation approach are then propagated through the simulation, and therefore, to the model outputs increasing the model prediction error (Wang et al., 2014; Chapagain et al., 2022). Site- and soil-specific empirical relationships were reported between the labile P pool in APSIM and different soil P tests (*e.g.* Wang et al., 2014; Micheni et al., 2004; Raymond et al., 2021), though the validity of extrapolating such relationships to other locations and cropping systems is still unknown.

An incorporation of soil test P values into process-based agricultural systems models such as APSIM will improve the understanding of soil P dynamics, and enable the quantitative soil P pool initialisation. The present study, using an optimisation framework that is akin to inverse modelling APSIM against crop P response data, quantitatively derived the most likely P modelling parameters to enable the initialisation of the labile P pool using soil test P values across a wide range of soils. Our objectives were to: (1) Validate the conceptual P modelling framework in APSIM using a long-term study (1997–2004) in Indiana, United States (US). This involved extending APSIM's parameterisation to simulate P responses in alfalfa (syn. lucerne, *Medicago sativa* L.); and evaluating model performance across various P fertilisation rates. (2) Optimise APSIM's labile P conditions to align modelled wheat (*Triticum aestivum* L.) yield responses with known Colwell-extractable P (Colwell P) response curves, for common grain-cropping soils in Australia. (3) Empirically link measured soil P values to APSIM's labile P pool for the studied soils. This research will assist in the understanding of P dynamics and support improved P management for greater P use efficiency in agricultural systems.

2. Materials and methods

2.1. The APSIM-SoilP module and its interaction with crop modules

The APSIM is a process-based agricultural systems model that simulates the growth and development of a wide range of crops, pastures and soil processes including water, C, N, and P dynamics under contrasting environments (climate × soil) and crop management practices. APSIM Version 7.10 simulates P dynamics in soil-crop systems through its SoilP module and crop modules (Probert, 2004; Delve et al., 2009). The crop modules contain information on the critical P concentrations in different organs of various crops, determining their P demands and the extent of P stress experienced, should P supply from the soil, modelled by the SoilP module, be inadequate to meet this demand.

The SoilP module (Probert, 2004; Delve et al., 2009) consists of three major P conceptual pools: (1) the labile P pool, which represents the pool of plant-available P, comprises both P in the soil solution and that loosely adsorbed on the soil surface that is available for crop uptake; (2) the stable inorganic P pool, which contains the P that is not readily available to crops during the growing season with first-order temperature-dependent processes assumed to determine loss or gain of availability relative to the labile P pool; and (3) the organic P pool that contains the P in soil organic matter (Fig. 1). The soil solution P is conceptualised as a secondary pool within the labile P pool in the APSIM SoilP module, with its equilibrium with the larger labile P pool controlled by a Freundich sorption equation, with coefficients ("a" and "b", which control the sorption capacity and the sorption rate respectively) that can be analytically derived through P sorption curves and are theoretically soil-specific. However, they are often adjusted empirically to match the dynamics of plant P uptake (*e.g.* Wang et al., 2014; Raymond et al., 2021). Users initialise the SoilP module by specifying the size of the labile P pool via labile P concentrations in various soil layers, while initial values for the rock P and banded P pools may also be set for each depth interval. In addition, several key input parameters must be defined: the rate of dissolution of rock P (default value of $0.2 year^{-1}$), the rate loss available (or r coefficient), and the root C:P ratio. The rate of dissolution of rock P governs the release of available P from any rock phosphate present at initialisation. The r coefficient modulates the transformation rate between the labile and unavailable P pools, and the root C:P ratio determines the carbon-to-phosphorus balance of the initial root biomass, thereby influencing both phosphorus mineralisation and immobilisation processes. The fertiliser module enables the addition of P fertiliser to the labile P pool of the SoilP, with the model differentiating between the types of fertiliser used and their placement methods. Banded and water-soluble forms of P fertilisers are considered more effective than broadcast non-water soluble fertilisers.

2.2. Data sources, model parameterisation and evaluation

We first investigated the effectiveness of the APSIM-SoilP module in representing soil P dynamics and simulating the P response of crops using data from a long-term P experiment cropped with alfalfa on two soils in Indiana, US as reported by Berg et al. (2020) in the Purdue University Research Repository (*Phosphorus and Potassium Influence on Alfalfa Nutrition, Version 2.0*). This was achieved by (1) calibrating the crop P parameters for alfalfa based on literature and field measurements of Berg et al. (2020) (Section 2.2.1) to enable P response of the APSIM-Lucerne module (Robertson et al., 2002); (2) using an optimisation function (Singer and Nelder, 2009) to initialise labile P pools for different mineral P fertilisation rates to increase Lin's concordance correlation coefficient (CCC) (Lin, 1989) of observed and modelled aboveground dry matter (DM) yields for alfalfa; and (3) assessing the agreement between observed and modelled plant biomass P content through graphical comparison and statistical analyses (Tedeschi, 2006). The empirical relationship between modelled labile P and measured soil Bray-2 P was examined. Section 2.2.2 details the US experimental data, simulation configuration, model parameterisation and evaluation of APSIM's capability to represent crop and soil P dynamics.

The optimisation function for labile P initialisation was subsequently used in an inverse-modelling approach to determine the labile P conditions that are likely to result in similar grain yield responses of wheat to measured Colwell P in different cereal-cropping soils in Australia. Inverse modelling is a technique used to estimate model parameters by comparing model outputs with observed data and iteratively adjusting the parameters until the model output matches the observations as closely as possible (Dokoohaki et al., 2018). Bell et al. (2013) derived empirical yield response curves for wheat for the major cropping soils of Australia using data from 1777 wheat P trial data between 1958 and 2011 from the Better Fertiliser Decisions for Crops (BFDC) database. The APSoil database contains parameterised soil profile information in Australia for the explicit use in APSIM (Dalgliesh et al., 2012). We undertook extensive simulations at the APSoil locations of these soil types by iteratively adjusting the labile P parameters to achieve wheat P yield responses as represented by the yield response curves in Bell et al.

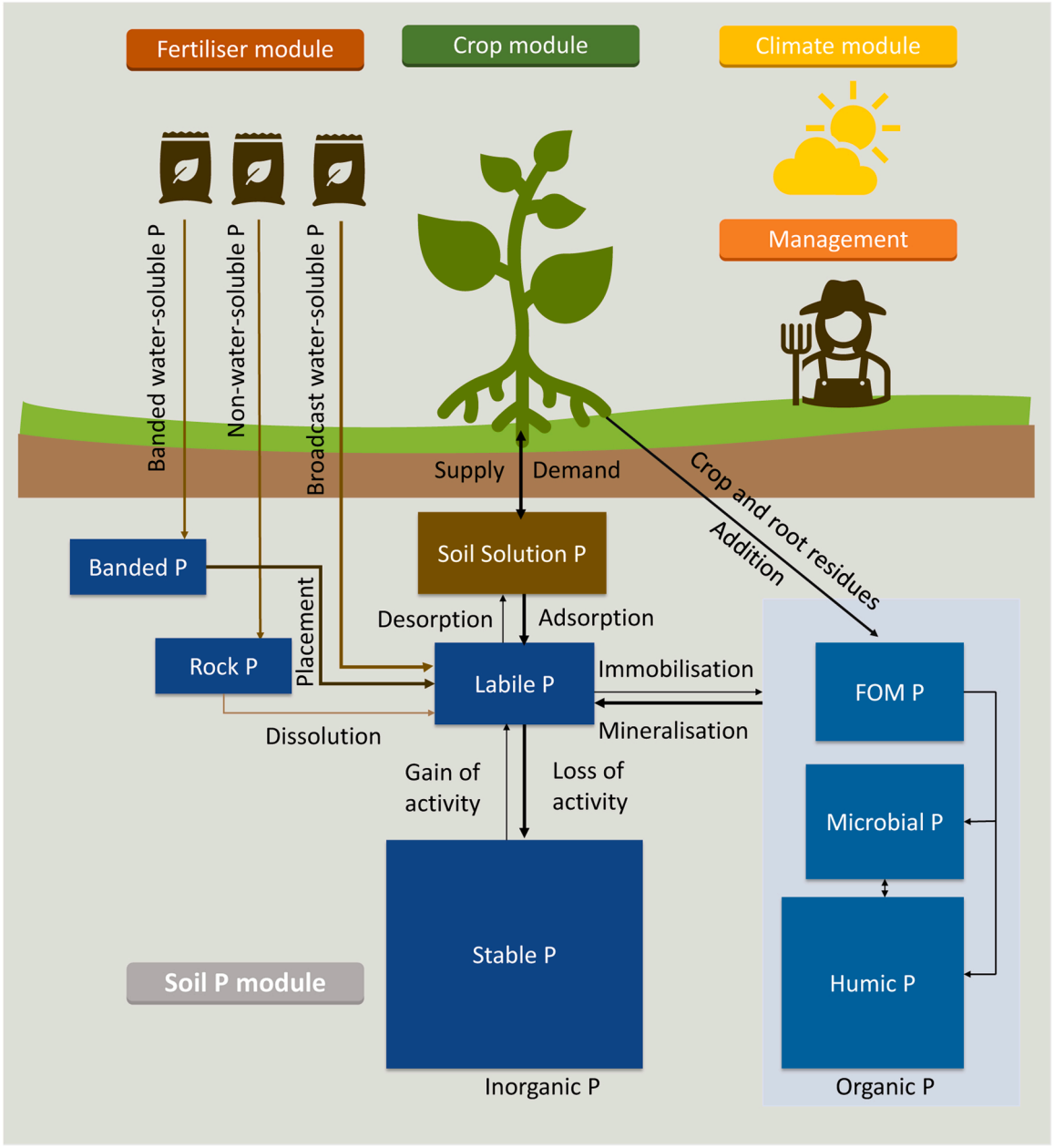

Fig. 1. Diagrammatic structure of soil phosphorus (P) pools in the Agricultural Production Systems sIMulator (APSIM). The boxes represent pools of the various forms of P, while the arrows represent translocations and transformations among these pools. Thick arrows represent the principal pathways. Arrows among the three organic pools also represent immobilisation/mineralisation pathways. FOM is fresh organic matter (adapted from Wang et al., 2014).

(2013). We then correlated Cowell P values to the modelled labile P empirically for each soil type. Section 2.2.2.1 describes the inverse-modelling approach, its application to the simulations, and the empirical model formulation for the estimation of labile P using Cowell P values.

As this study focused primarily on the interaction between labile P values and the sorption capacity coefficient "a" to ensure a conservative approach that enables quantitative initialisation of labile P values based on measured soil P values across wide geographical regions, the sorption coefficient *b* was set to a value of 0.7 *i.e.*, the default value in APSIM-SoilP (Probert, 1985). The *r* coefficient was set to 0.3, consistent with values reported by Wang et al. (2014) and used as a baseline in Raymond et al. (2021). The root C:P ratio was set at 200, consistent with that used in previous studies (Micheni et al., 2004; Delve et al., 2009; Wang et al., 2014; Raymond et al., 2021). The rate of dissolution of rock P was set to 0.2year^{-1}. The rock P content and banded P content at each soil layer were initialised to 0.

2.2.1. Crop P parameterisation

The P concentration ranges of plant organs at different growth stages are used in APSIM to calculate crop P demand. The parameter values used in the simulations of this study are given in Table 1. The P concentrations for alfalfa were derived based on Lu et al. (2016), Lu et al. (2019), Lu et al. (2020), He et al. (2017), combined with the P concentrations measured in the experiment (Berg et al., 2020). The original values were specified for the start of each growth stage and interpolated between stages. For wheat, P concentration limits followed Wang et al. (2014).

2.2.2. Long-term P trial, Indiana, United States

A field experiment was conducted from 1997 to 2004 on two soils at Throckmorton Purdue Agricultural Center (TPAC), Indiana, US, to study

Table 1
Minimum (min) and maximum (max) phosphorus concentrations (% dry matter) of plant organs used in APSIM modelling.

Plant organs	Emergence		Flowering		Grain filling		Physiological maturity	
	min	max	min	max	min	max	min	max
Alfalfa[a]								
Leaf	0.25	0.40	0.115	0.50			0.15	0.28
Stem	0.25	0.35	0.065	0.35			0.12	0.20
Root	0.04	0.18	0.04	0.18			0.04	0.15
Pod	0.00	0.00	0.15	0.25			0.15	0.25
Meal	0.00	0.00	0.30	0.45			0.30	0.45
Oil	0.01	0.01	0.01	0.01			0.01	0.01
Wheat[b]								
Leaf	0.20	0.60	0.08	0.16	0.07	0.13	0.02	0.08
Stem	0.20	0.60	0.08	0.16	0.07	0.13	0.02	0.08
Root	0.10	0.22	0.08	0.16	0.07	0.13	0.02	0.08
Chaff			0.08	0.16	0.07	0.13	0.02	0.08
Grain					0.20	0.30	0.20	0.30

[a] Values derived based on Lu et al. (2016), Lu et al. (2019), Lu et al. (2020), He et al. (2017) and the measured values in Berg et al. (2020).
[b] Values adapted from Wang et al. (2014).

the influence of P and potassium (K) nutrition on alfalfa (Berg et al., 2020). The experiment details and findings were discussed extensively in Berg et al. (2005), (2007), 2009); Lissbrant et al. (2009) and Woodson et al. (2013). Alfalfa cultivar Pioneer Brand "5454" was sown in April 1997. The fertilisation treatments consisted of four annual P rates (0, 25, 50, and 75 kg ha^{-1}) and five K rates (0, 100, 200, 300, and 400 kg ha^{-1}) arranged in four replicates of a randomised complete block design, with two replicates placed on a Drummer silty clay loam (fine-silty, mixed, super-active, mesic Typic Endoaquoll; World Reference Base [WRB] equivalent: Gleysols) and the other two placed on a Lauramie silt loam (fine-loamy, mixed, active, mesic, Mollic Hapludalf; WRB equivalent: Luvisols). Four forage harvests occurred each year at approximately 30-day intervals beginning in late May from 1998 to 2004. Fertilisers (both P and K) were applied in split applications, with one-half the annual amount surface broadcast after the first forage harvest in late May, and the remainder surface broadcast after the last forage harvest in mid-September from 1998 to 2004. Chemical control of pests occurred when threshold limits were surpassed. As alfalfa is a perennial, no annual re-sowing or soil tillage was implemented. Soil test P and K levels were monitored following each growing season. In 1998 and 1999, soil tests were conducted after the final harvest and the second fertilisation, in October 1998 and November 1999, respectively for the 0–20 cm depth. From 2000 to 2004, soil tests were conducted using soil samples at 5 cm increments from 0 to 20 cm in conjunction with each harvest. Soil P availability was estimated using the Mehlich III extraction procedure and then interpolated to Bray-2 P (Denning et al., 1998). As only Bray-2 P values were reported in Berg et al. (2020), these values were used for subsequent comparisons with APSIM labile P estimates in this study.

2.2.2.1. APSIM configuration. Since APSIM 7.10 has no ability to model K dynamics, we only retained experimental results from maximum K rate application treatments (*i.e.* 400 kg ha^{-1} K) to use in our simulations, with the assumption that K deficiency was not present in these K treatments. Alfalfa cultivar Grasslands Kaituna was selected in APSIM to represent the winter-dormant Pioneer "5454" sown (as this cultivar behaves like a winter-dormant cultivar; Pembleton and Sathish, 2014). Simulations for the experimental period (1997–2004) were undertaken using a daily time-step of APSIM with the two soil profiles characterised following Ojeda et al. (2017) (Supplementary Table S1). The simulation start date was April 1, 1997, with alfalfa sown on April 15, 1997, at a sowing density of 1000 plants m^{-2} at a sowing depth of 15 mm and row spacing of 150 mm. However, as APSIM-Lucerne represents populations in terms of stems rather than individual plants, and each plant typically produces 5–10 stems depending on stand age, this corresponds to an estimated plant density of 100–200 plants m^{-2}. It is also important to note that the APSIM-Lucerne module is not sensitive to row spacing, meaning it does not impact model outputs. The four harvests were arbitrarily set to May 25, June 30, August 10, and September 15 as the exact dates of harvests were unavailable, and P was applied on May 26 and September 16 until 2004. The model was run continuously without resetting soil variables for the entire experimental period.

2.2.2.1.1. Alfalfa winter dormancy rules. The manager component in APSIM allows users to dynamically control their simulations through scripted conditional rules. To ensure that the APSIM-Lucerne model captured the process of winter dormancy, we initialised temperature and photoperiod rules using a crop manager script as described in Pembleton et al. (2011) and Ojeda et al. (2016). We then optimised the parameters using the Nelder-Mead method (Singer and Nelder, 2009). This method allows efficient direct optimisation of the response function by comparing function values, which is suitable for situations where derivatives are difficult to compute, such as ours, when a complex agricultural systems model is used (Gao and Han, 2012). This involved iteratively optimising the set of parameters to improve the agreement between the observed aboveground DM yields and corresponding modelled aboveground DM yields using data from both soils for the maximum P treatment (*i.e.* 75 kg ha^{-1}) with the SoilP module disabled. This assumes that under the maximum P treatments, the crops were under a non-P-limiting environment.

2.2.2.1.2. SoilP calibration and harmonisation. We initialised the P sorption capacities of the Drummer and Lauramie soils with respect to their clay contents, with the assumption that labile soil P concentration decreases while P sorption increases with soil depth (Wang et al., 2014). For each soil, we iteratively adjusted the initial labile P for the top soil layer with the Nelder-Mead optimisation so that the agreement between modelled aboveground DM yield and observed aboveground DM yield was maximised, while labile P for the remaining soil layers were initialised with a value of 1 mg kg^{-1}. We selected 0–20 cm as the target depth interval to derive empirical relationships between field-measured soil Bray-2 P values and the labile P pool values in APSIM, as Bray-2 P were measured to 20 cm in the field experiment. We retained the measured Bray-2 P values from 1998 and 1999, and harmonised the 5-cm Bray-2 P increments from 2000 to 2004–0–20 cm using an equal-area quadratic spline (EA-spline) (Bishop et al., 1999). In addition, the surface soil depths for the characterised soil profiles used in APSIM (Ojeda et al., 2017; Supplementary Table S1) were 0–23 cm for Drummer and 0–20 cm for Lauramie. Therefore, for Lauramie soil, the labile P output from APSIM at the soil sampling dates for the top layer, *i.e.* 0–20 cm, was directly used. For Drummer soil, APSIM-modelled labile P values were first harmonised across the full soil profile depth using the EA-spline interpolation method, and the values corresponding to the 0–20 cm depth were retained for analysis.

2.2.3. Better Fertiliser Decisions for Crops National Database, Australia

Bell et al. (2013) interrogated data from 1777 wheat field treatment series from 1958 to 2011 held in BFDC National Database in Australia and developed empirical relationships between relative grain yield (RY) of wheat and the Colwell P measured in surface soil (0–10 cm) for the eight major soil types within five Australian Soil Orders (Isbell and the National Committee on Soil and Terrain, 2021) (Fig. 3). Table 2 shows their respective Soil Taxonomy classification (Isbell and the National Committee on Soil and Terrain, 2021). We applied an inverse-modelling approach to the APSoil locations of these soil types (Fig. 2) to determine the labile P conditions that were likely to result in similar yield responses of wheat to the Colwell P in surface soils as illustrated in Fig. 3, then correlated the Colwell P to the APSIM-modelled surface and subsurface labile P empirically. Fig. 4 illustrates our methodology in detail using Red Chromosols as an example.

The relative yields ($RY_{1:n}$, %) to Colwell P of 1 to n, where n is the largest integer of the Colwell P value whose corresponding relative yield

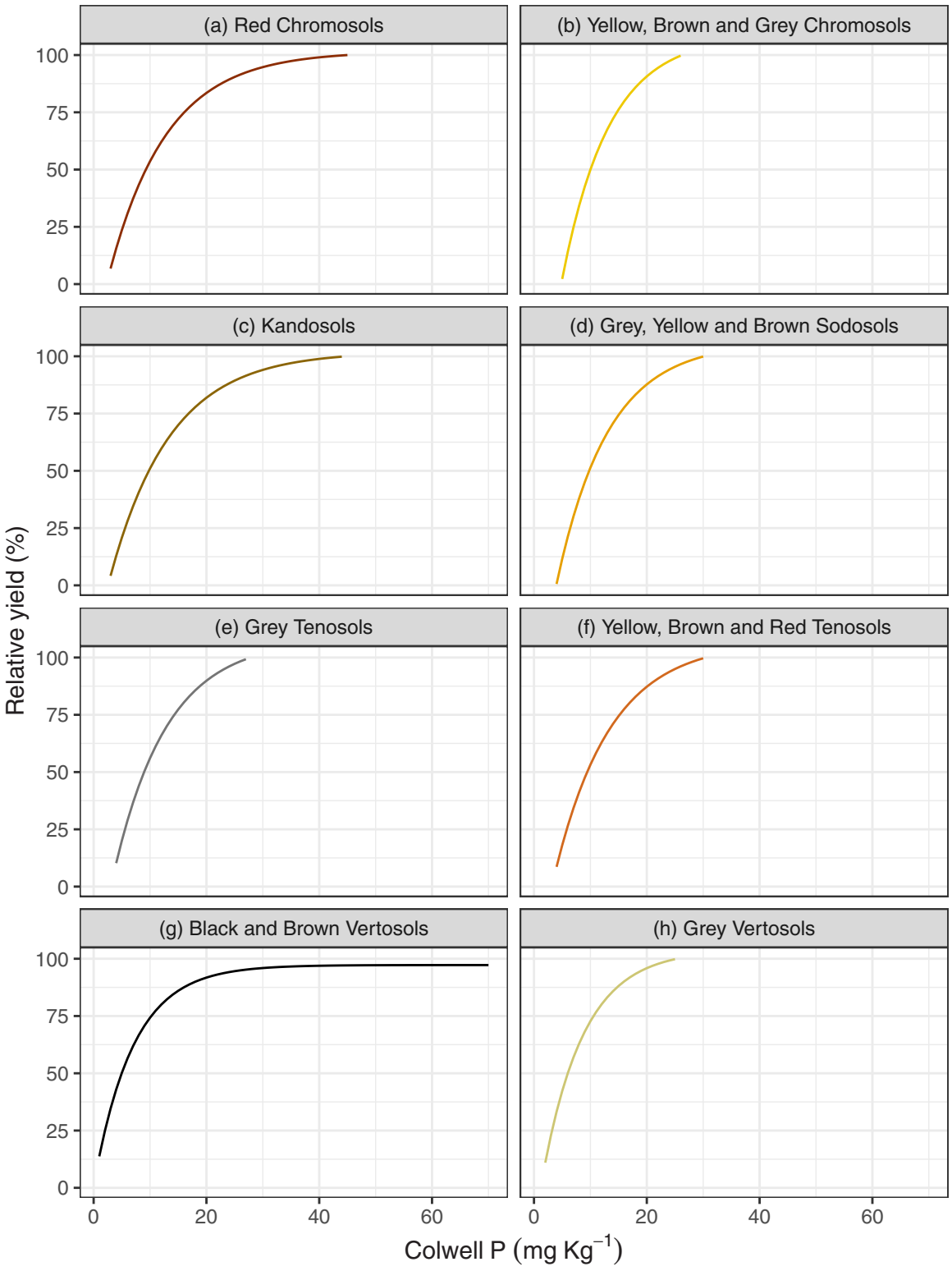

Fig. 3. Relationships between relative wheat grain yield (as a percentage of maximum) and Colwell-extractable P in 0–10 cm soil depth by soil types (Bell et al., 2013).

is ⩽100 % were extracted for the wheat P yield response curve of Red Chromosols. For all APSoil sites, daily historical climate data (1958–2011), including daily maximum and minimum air temperatures, solar radiation, and rainfall were sourced from SILO patched database (Jeffrey et al., 2001, https://silo.longpaddock.qld.gov.au/, accessed on March 30, 2020). The P sorption capacities of the five soil orders were parameterised based on the median P buffering capacities (PBC) of the surface soils described in Burkitt et al. (2002). Since P sorption generally increases with soil depth, subsurface P sorption capacity was assumed to be at 1.5 times that of surface soil and all subsoil depths at 1.8 times the surface soil sorption (Table 2). Simulations were conducted over twenty randomly selected years between 1958 and 2011 at each APSoil

Table 2
Phosphorus sorption capacities used for the five Australian soil orders and their respective Soil Taxonomy and World Reference Base classification.

Australian Soil Classification	Chromosols	Sodosols	Tenosols	Kandosols	Vertosols
Soil Taxonomy[a]	Alfisols some Aridisols	Alfisols Aridisols	Inceptisols Aridisols, Entisols	Alfisols Ultisols, Aridisols	Vertisols
World Reference Base	Abruptic Luvisols/Lixisols	Solonetz, Abruptic Luvisols, Planosols	Cambisols, Leptosols Plinthosols	Ferralsols Luvisols, Lixisols	Vertisols
Depths (cm)					
0–15	50	10	30	109	80
15–30	75	14	45	163	120
30–60	89	18	54	197	143
60 and lower	89	18	54	197	143

[a] These correlations are approximate as differentiating criteria often differ among soil classification systems (Isbell and the National Committee on Soil and Terrain, 2021).

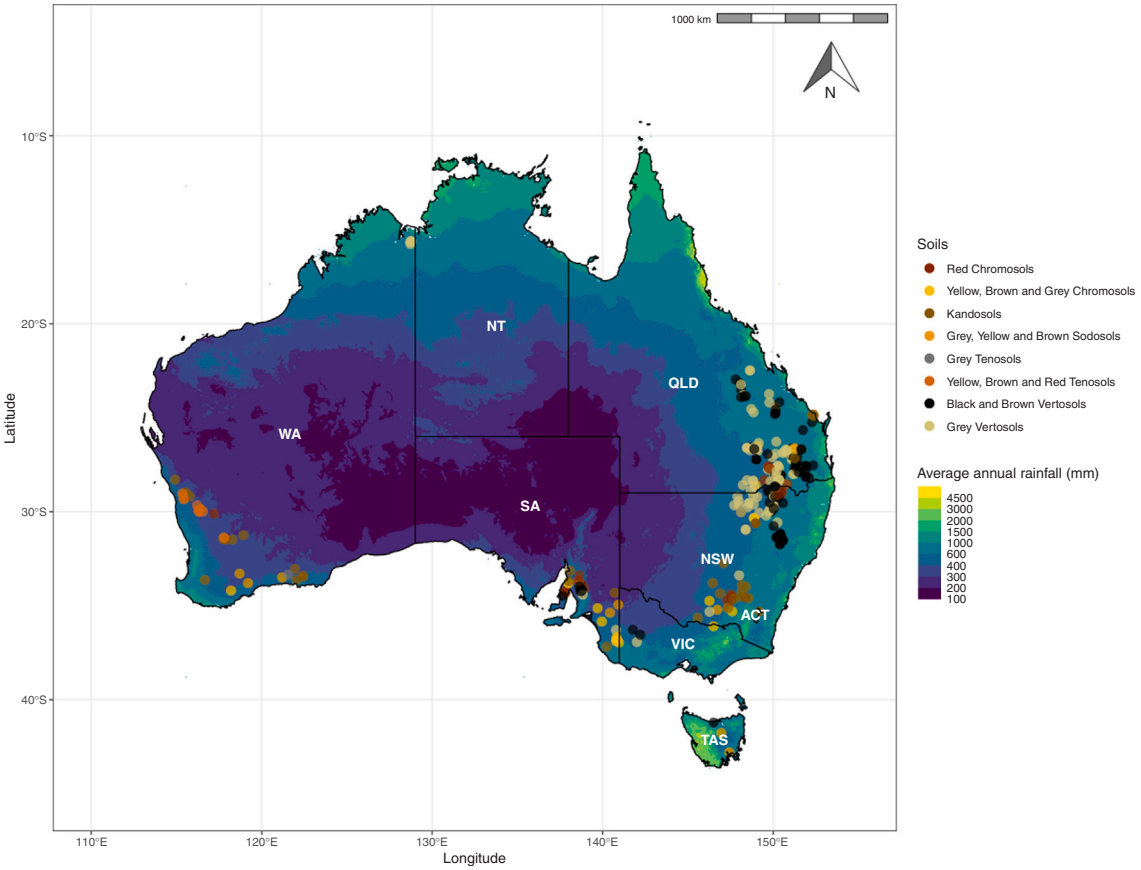

Fig. 2. Distribution of mean cumulative annual rainfall across Australia and APSoil profile locations for the eight soil types investigated.

location. The simulations modelled annual wheat crops, initiated on December 1 of the preceding year with soil water levels reduced to the crop lower limit. This assumes that the soil profile's plant-available water was depleted at the end of the season by a prior winter crop. The sowing window was set from 26 April to 15 July, during which wheat was sown if accumulated rainfall over three days exceeded 15 mm. If this rainfall criterion was not met by the end of the sowing window, the crop was sown on the final day, 15 July. The wheat cultivar Hartog was planted at a density of 150 plants m^{-2}, with a sowing depth of 30 mm and a row spacing of 250 mm. To prevent nitrogen stress, 500 kg ha^{-1} N was applied as urea fertiliser at the time of sowing (Meier et al., 2021). Using the check variety Hartog with a consistent management regime across the modelled temporal periods ensures a focused analysis of how the initialisation of labile P values in APSIM for soils with different P sorption characteristics interacts with climatic variables to influence yield responses.

For the US experiment-based study, we established a relationship between Bray P and the APSIM-modelled labile P using the mean APSIM-modelled labile P values (mg kg^{-1}) for the months where soil samples were taken to measure soil Bray P, then fitting various linear and non-linear regressions, including log-logistic functions, Weibull functions, asymptotic regressions, and Michaelis-Menten functions with different parameters, to the Bray P and labile P values at 0–20 cm soil depth interval. The best model was chosen using the Akaike Information Criterion (AIC, Sakamoto et al. 1986). Leave-one-soil-out cross-validation was performed to assess the predictive accuracy of the chosen model. For the Australian simulation-based study, relationships between Colwell P and APSIM-labile P across different soil types were analysed by applying the same regression models as in the US study to the Colwell P values in the 0–10 cm soil depth and labile P values for the surface and subsurface soil depths, which are the most important two soil depths for P modelling initialisation in APSIM. The model with the lowest AIC was selected. Five-fold cross-validation was performed for the APSoil locations associated with each soil type, in which all the APSoil locations for

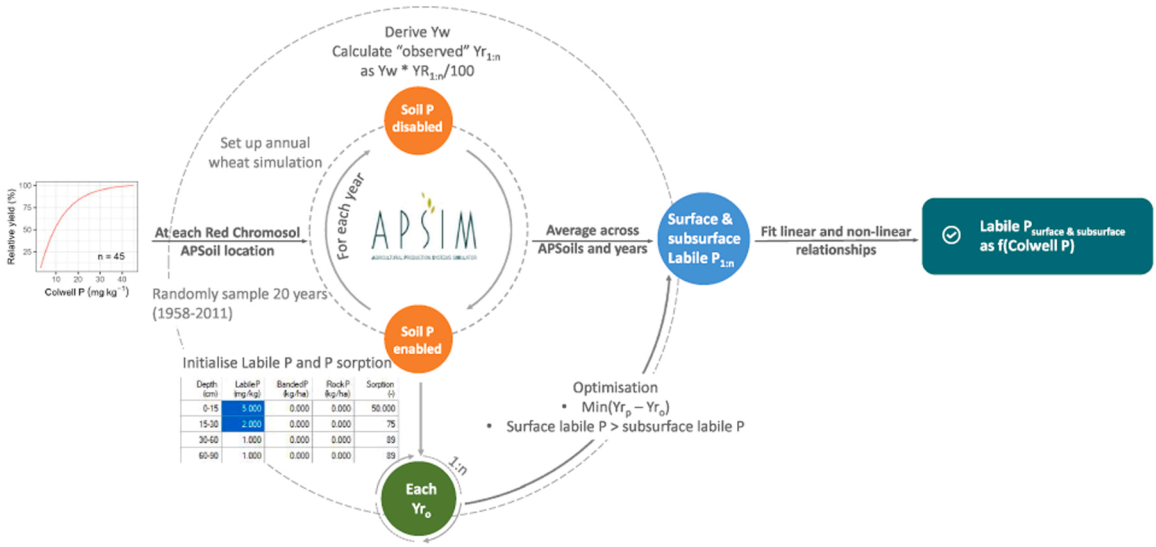

Fig. 4. Inverse-modelling framework to derive empirical relationships between surface and subsurface labile P in APSIM and Colwell-extractable P (Colwell P) using Red Chromosols as a demonstration. $RY_{1:n}$ represent the corresponding relative yield (%) to Colwell P of 1 to n, Y_w represents the water limited yield potential (kg ha^{-1}) for the simulation year at the APSoil location, *i.e.* the maximum attainable yield under rain-fed conditions; therefore at Y_w, RY is 100 %. $Yr_{1:n}$ represents the expected yield (kg ha^{-1}) for Colwell P of 1 to n, while Yr_o represents the yield derived based on Y_w and RY, and Yr_p represents APSIM-predicted yield by optimising surface and subsurface labile P values so that difference between Yr_o and Yr_p is minimised. Surface and subsurface labile P values are indicated in the selected cells (blue) of the APSIM Soil P interface with the P sorption capacities parameterised based on Burkitt et al. (2002). Simulations were repeated for 20 randomly sampled years between 1958 and 2011 (small circle) at each APSoil location of the soil type—Red Chromosols (big circle).

a soil type were divided into five folds, where one fold is reserved for model validation while the remaining folds are used for training. This process is repeated until each fold has been used as the validation set.

3. Results

3.1. Empirical relationships between measured P fractions and labile P

3.1.1. Empirical relationship between Bray P and labile P

A Weibull2 function $y = 0 + (102.26 - 0)(1 - \exp(-\exp(1.62(\log(x) - \log(20.73)))))$ as described by Seber and Wild (1989) expressed in the generic form (Equation 1) was considered the best fit for correlating Bray P and labile P (Fig. 5, Table 3). This parameterisation shifts the standard curve $f(x;\delta) = 1 - \exp(-x^{\delta}), \quad x > 0$ vertically. The labile P y increases sharply from c, 0–64.66 mg kg^{-1} when Bray-2 P x increases from 0 to the value of e: 20.73 mg kg^{-1}, then asymptotically approaches the value of d: 102.26 mg kg^{-1} with the steepness of the transition from 0 to d being controlled by the parameter b: 1.62. A larger b makes transition sharper, while a smaller b makes it more gradual. The Leave-one-soil-out cross-validation showed an R^2 of 0.87 and a CCC of 0.92 for the labile P and Bray P relationship. The b, d, and e fitted to Drummer data is 1.80, 96.54 and 20.01 respectively and the b, d, and e fitted to Lauramie data are 1.45, 115.61 and 22.97 respectively, while c = 0 (Table 3).

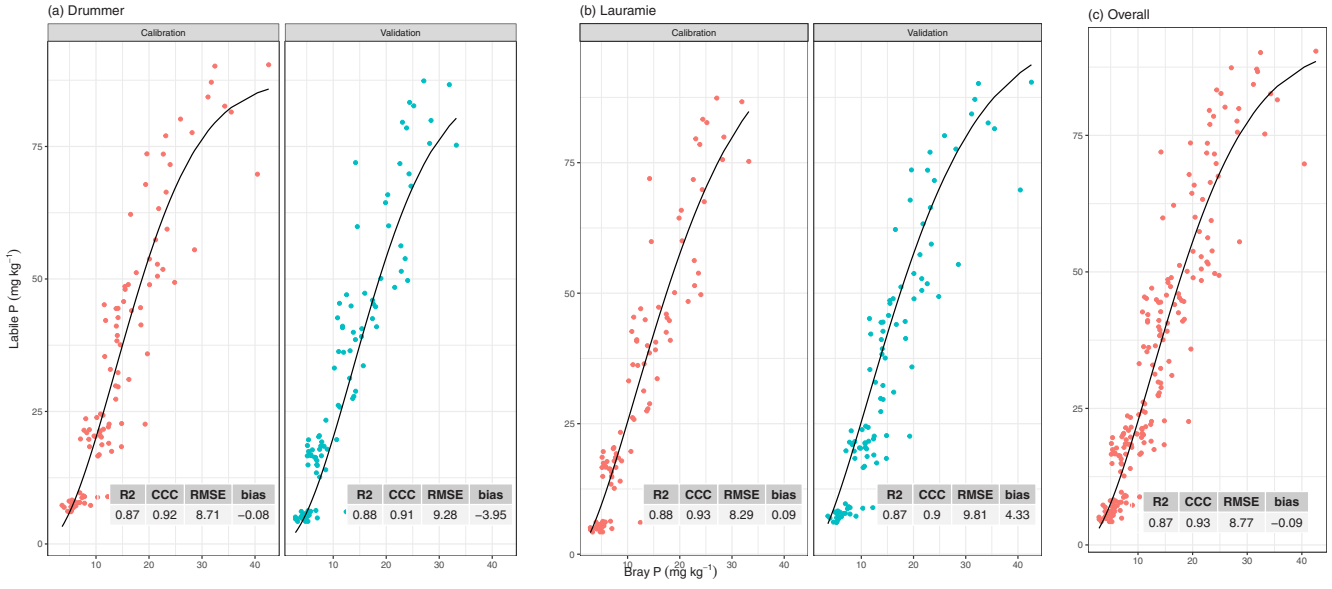

Fig. 5. Leave-one-soil-out cross-validation of measured Bray phosphorus (P) concentrations and modelled labile P concentrations of (a) Drummer soil as calibration (b) Lauramie soil as calibration, and (c) non-linear correlation derived based on data from both soils.

Table 3
Estimated model parameters for different soil types and layers, linking measured Bray-2 P values (mg kg^{-1}) from long-term alfalfa experiments (United States) and discrete Colwell P values (mg kg^{-1}) from Colwell P-wheat yield response curves in the Better Fertiliser Decisions for Crops Database (Australia) to APSIM-modeled labile P (mg kg^{-1}). The table includes the fitted function type and associated parameter values (b, c, d, e).

Soils	Depth layer	b	c	d	e	Function
			United States			
Drummer	0–20 cm	1.80	0	96.54	20.01	Weibull2
Lauramie	0–20 cm	1.45	0	115.61	22.97	Weibull2
Overall	0–20 cm	1.62	0	102.26	20.73	Weibull2
			Australia			
(a) Red Chromosols	Surface	−0.94	2.47	65.03	17.57	Weibull1
	Subsurface	−0.55	1.72	166.60	92.73	Weibull1
(b) Yellow, Brown and Grey Chromosols	Surface	−0.38	0.00	338.14	143.25	Weibull1
	Subsurface	−0.46	1.74	307.74	143.62	Weibull1
(c) Kandosols	Surface	0.63	−9.07	735.13	468.02	Weibull2
	Subsurface	0.85	0.00	401.49	362.68	Weibull2
(d) Grey, Yellow and Brown Sodosols	Surface			1009.21	613.25	Michaelis-Menten
	Subsurface	1.29	1.10	396.13	201.75	Weibull2
(e) Yellow, Brown and Red Tenosols	Surface	1.46	5.47	4085.72	477.20	Weibull2
	Subsurface	1.43	2.80	1412.56	349.94	Weibull2
(f) Grey Tenosols	Surface	−4.07	5.08	44.08	12.65	Log-logistic
	Subsurface	−2.54	2.16	40.48	17.33	Log-logistic
(g) Black and Brown Vertosols	Surface	−0.69	2.31	97.40	26.22	Weibull1
	Subsurface	1.17	0.59	163.20	131.29	Weibull2
(h) Grey Vertosols	Surface	−1.28	4.34	59.29	8.55	Weibull1
	Subsurface	−0.46	1.88	198.82	99.77	Weibull1

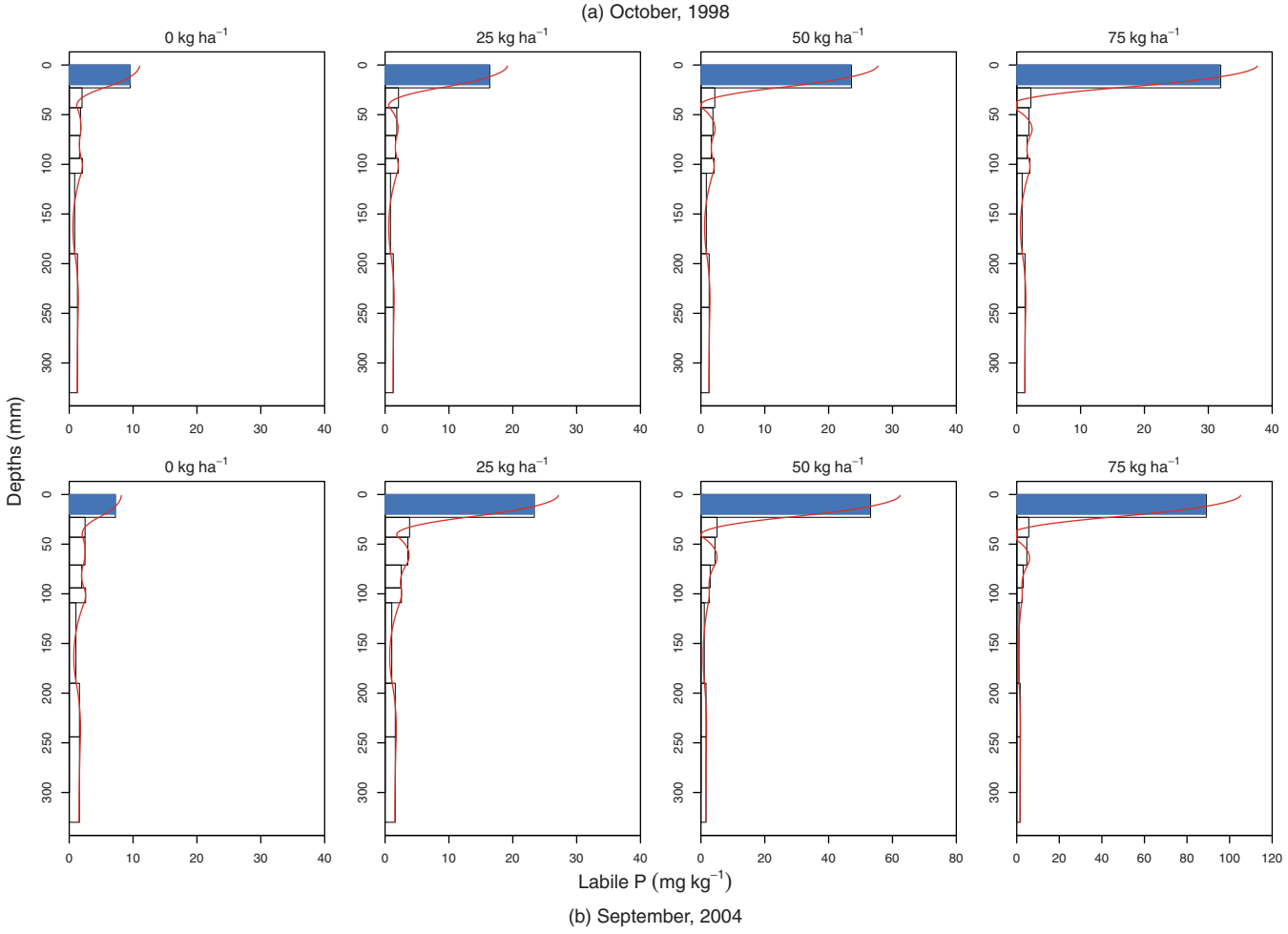

Fig. 6. Fitted equal-area quadratic spline at 1-cm steps (red line) to the labile P (bars) modelled by APSIM for the Drummer soil at (a) the first soil sampling in October 1998 and at (b) the last soil sampling in September 2004. The solid navy bar at 0–20 cm represents the harmonised soil labile P concentration used for empirical correlation to measured Bray P at the same depth.

$$y = c + (d - c)(1 - \exp(-\exp(b(\log(x) - \log(e))))) \quad (1)$$

where x is the independent variable, here the APSIM-modelled labile P initialisation values (mg kg^{-1}) for the 0–20 cm layer; y is the dependent variable, here the measured Bray-2 P values for the 0–20 cm layer; c represents the minimum possible value of y; d determines the upper limit of y as $x \to \infty$; b controls how quickly the function transitions from c to d; and e adjusts the location of the inflection point, determining at what x the function transitions most rapidly.

3.1.1.1. Harmonisation of labile P for Drummer soil. Fig. 6 showed the fitted EA-splines at the first soil sampling in October 1998 and at the last soil sampling in September 2004 for the Drummer soil. This was performed at all sampling dates to enable the derivation of harmonised soil labile P concentrations at our target soil depth interval (0–20 cm). The labile P concentrations increased in the surface soil due to fertilisation in 1998. This increase was enhanced after 6 years. The 50 kg ha^{-1} and the 75 kg ha^{-1} treatments doubled and tripled their labile P concentrations in the surface soils respectively in 2004 compared to in 1998. Under no P fertilisation, however, the labile P concentrations remained low and slightly decreased over the course of the experiment.

3.1.2. Empirical relationship between Colwell P and labile P

The fitted empirical relationships between Colwell P in the 0–10 cm soil depth and labile P for the surface and subsurface soil layers in APSIM are shown for different cereal-cropping soils in Australia (Fig. 8, Table 3). A two-parameter Michaelis-Menten model $y = \frac{d}{1+\left(\frac{e}{x}\right)}$ (AIC: 66.23) was considered the best fit for the surface soil layer of Grey, Yellow and Brown Sodosols. A four-parameter log-logistic function of the form $y = c + \frac{d-c}{1+\exp(b(\log(x)-\log(e)))}$ was considered the best fit for both the surface and subsoil surface layers of Grey Tenosols. Of all other soils, either a Weibull1 (Equation 2) or a Weibull2 (Equation 1) function was considered the best fit for the surface and subsurface layers. A Weibull1 parameterisation shifts the standard curve horizontally rather than vertically compared to the Weibull2 parameterisation and when b is negative, y increases as x increases (Fig. 7). Either a Weibull1 or Weibull2 function was also considered the top three best fits for both layers of Grey Tenosols and for the surface layer of Grey, Yellow and Brown Sodosols. The average AIC difference between the best fit and the Weibull fit was 1.03. This very small difference suggested that a Weibull distribution can also adequately represent the relationship between Colwell P in the 0–10 cm soil depth and APSIM-modelled labile P for these soils. A five-fold cross-validation showed that the fitted models exhibit high predictive accuracy (R^2 mean: 0.97, median: 0.98; CCC mean: 0.91, median: 0.94) and low overall error (RMSE mean: 4.12 mg kg^{-1}, median 2.44 mg kg^{-1}) and minimal systematic bias (bias mean: −0.01 mg kg^{-1}, median: 0.02 mg kg^{-1}). Table 4 illustrates the performance of the cross-validation for each of the soil types studied. The surface layers of Kandosols, Yellow, Brown and Red Tenosols and Grey Tenosols appeared to perform slightly worse than the other soils, with an average CCC of 0.82, 0.83 and 0.81 respectively and an average RMSE of 17.08, 10.3 and 8.37 mg kg^{-1} respectively.

$$y = c + (d - c)\exp(-\exp(b(\log(x) - \log(e)))) \quad (2)$$

where x is the independent variable, here the APSIM-modelled labile P initialisation values (mg kg^{-1}) either in surface or subsurface layers of the APSoil profiles for a specific soil type; y is the dependent variable, here the discrete Colwell P values (mg kg^{-1}) extracted from Colwell P-wheat yield response curves of BFDC database for the corresponding soil type; c represents the minimum possible value of y; d determines the upper limit of y as $x \to \infty$; b controls how quickly the function transitions from c to d; and e adjusts the location of the inflection point, determining at what x the function transitions most rapidly. Fig. 8.

Table 5 shows critical labile P concentrations corresponding to the critical Colwell P concentrations at 0–10 cm depth interval reported in

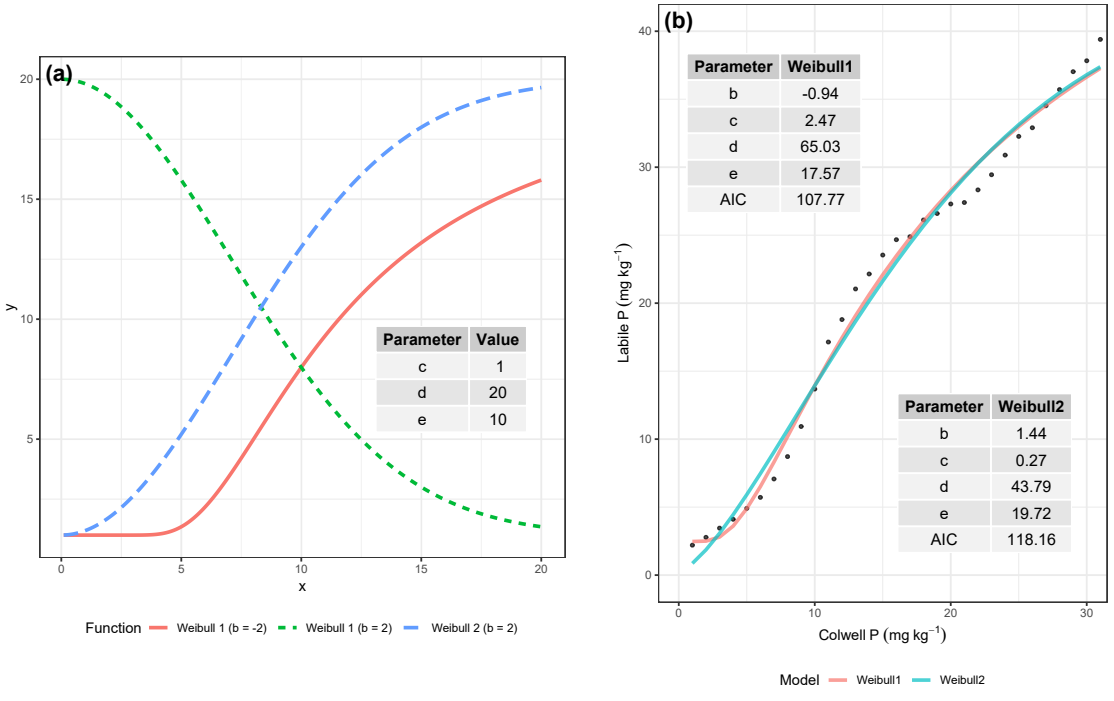

Fig. 7. Comparison of Weibull function behaviours and model fittings. (a) Displays the Weibull function responses for different shape parameters (b=2 and b= − b influence the function shape, with increasing b leading to steeper transitions, and a negative b changes Weibull1 from a decay function to growth function. (b) Presents the fitted Weibull1 and Weibull2 functions for Red Chromosols in Australia, where Colwell P (mgkg^{-1}) is correlated with APSIM-modelled labile P (mgkg^{-1}) for the surface layer. Model parameter values, including shape and scale parameters (b,c,d,e), along with Akaike Information Criterion (AIC) values, are provided in the annotated tables. The comparison highlights differences in model fits and parameter influence on curve behaviour.

Table 4
Summary of averaged validation statistics across the five-fold cross-validation, including R^2, Lin's Concordance Correlation Coefficient (CCC), Root Mean Square Error (RMSE), and bias for different Australian soil types. Surface and subsurface layers correspond to the top two depth layers in APSIM for labile P initialisation.

Soil	Layer	R2	CCC	RMSE	bias
(a) Red Chromosols	Surface	0.98	0.95	2.08	0.11
	Subsurface	1.00	0.96	0.79	0.07
(b) Yellow, Brown and Grey Chromosols	Surface	0.98	0.90	4.13	0.25
	Subsurface	0.99	0.93	1.93	0.28
(c) Kandosols	Surface	1.00	0.82	17.08	−0.74
	Subsurface	1.00	0.96	1.81	0.03
(d) Grey, Yellow and Brown Sodosols	Surface	0.98	0.93	2.51	−0.04
	Subsurface	0.99	0.94	1.78	0.15
(e) Yellow, Brown and Red Tenosols	Surface	0.94	0.83	10.30	0.15
	Subsurface	0.98	0.94	2.37	−0.15
(f) Grey Tenosols	Surface	0.91	0.81	8.37	−0.23
	Subsurface	0.85	0.86	4.19	0.06
(g) Black and Brown Vertosols	Surface	0.99	0.95	2.52	−0.01
	Subsurface	1.00	0.96	0.88	−0.00
(h) Grey Vertosols	Surface	0.98	0.93	4.04	−0.10
	Subsurface	0.99	0.95	1.09	0.00

Bell et al. (2013) to achieve 80 %, 90 % and 95 % relative yields for each soil group. Red Chromosols and Kandosols have the same critical Colwell P concentrations. However, the labile P pool in APSIM for Kandosols needs to be initialised with much higher values compared to Red Chromosols to achieve the same relative yields due to the higher P sorption capacities of Kandosols (Table 2). Similar trends are also observed between Grey, Yellow and Brown Sodosols and Yellow, Brown and Red Tenosols, of which higher P sorption capacities were used for Tenosols compared to Sodosols (Table 2). Within the same soil orders where we had used the same P sorption capacities in our simulations, Yellow, Brown and Grey Chromosols require higher labile P values in both surface and subsurface APSIM soil layers to achieve the same relative yields compared to Red Chromosols though their critical Colwell P concentrations at 80 %, 90 % and 95 % relative yields were all lower than Red Chromosols. This is attributed to the steeper rate of change in relative yields in response to Colwell P for Yellow, Brown and Grey Chromosols than that for Red Chromosols (Figure 3). A similar trend is also observed between Grey Vertosols and Black and Brown Vertosols. On the other hand, Yellow, Brown and Red Tenosols require higher critical Colwell P concentrations and higher labile P values to achieve the same relative yields compared to Grey Tenosols.

3.2. P dynamics modelling in APSIM

3.2.1. Alfalfa

3.2.1.1. Winter dormancy rules of Alfalfa. Using the optimisation function to parameterise the photoperiod threshold and temperature thresholds for entry and exit from alfalfa dormancy (Table 6) achieved reasonable accuracy with an overall predictive accuracy of $R^2 = 0.71$, CCC = 0.78, RMSE = 939.54 and bias = −383.6 kgha^{-1} between observed and modelled DM yields for the maximum P treatment on both soils, at TPAC, Indiana, US. With this winter dormancy setting, the model generally over-predicted DM yields for the first harvests and under-predicted DM yields for the subsequent harvests (Fig. 9). This is particularly evident in the last harvests in September which were always underestimated, contributing to the overall underestimation of DM production (Fig. 11). A higher agreement was achieved on the Lauramie soil compared with the Drummer soil (Fig. 9). This winter dormancy rule thus enables the APSIM model to simulate seasonal variability in DM yields of alfalfa over the seven-year experimental period.

3.2.1.2. Response of alfalfa growth to P addition. The seasonal patterns of alfalfa aboveground DM yields under several P fertilisation rates were satisfactorily modelled by APSIM (Figure 10, left panel; Figure 11 (a)). The DM yields from the Drummer site were generally underestimated (bias = −213.95 kg ha^{-1}) while those from the Lauramie site were overestimated (bias = 96.74 kg ha^{-1}). Across both sites, APSIM achieved a prediction accuracy of $R^2 = 0.57$, CCC = 0.74, RMSE = 1033.4 and bias = -58.61 kg ha^{-1}. Reasonable prediction accuracy for the DM yields each year was also achieved except in 2002 (Table 7). The model accuracy on the seasonal patterns of P contents in plant biomass of alfalfa for the different P fertilisation rates was less accurate compared to the DM yields (Fig. 10, right panel, Fig. 11 (b)). The APSIM model achieved an overall prediction accuracy of $R^2 = 0.43$, CCC = 0.74, RMSE = 4.14 and bias = 1.89 kg ha^{-1} with better performance on the Drummer soil compared with the Lauramie soil. The model represented the effects of different P fertilisation rates on alfalfa production without significant differences in its ability to simulate crop responses under both low and high P fertilisation rates, indicating it can reliably simulate crop responses to varying levels of soil P availability and fertilisation rates.

4. Discussion

The APSIM-SoilP module was developed to work with APSIM crop modules to simulate crop response to P availability in soils. Availability of P is determined by sorption/desorption processes and the total amount of P available. There have been no previous studies on whether the model is able to predict growth response to P additions for alfalfa. Our parameterisation for alfalfa based on previous literature and the subsequent simulation results for their growth indicate, using an inverse modelling approach to calibrate the model, APSIM was able to adequately predict alfalfa growth, DM yield, P uptake and plant biomass P content in response to different fertiliser P inputs and amounts of residual P in two different soils in a detailed long term experiment. The consistent under-estimation of DM yields by the model at the last harvests in September can be attributed to the parameterisation of the winter dormancy rule which defined crop growth stages based on the temperature change on a daily drop or rise, which does not reflect the true conditions in the field. We also assumed that the highest P fertilisation rate treatment of 75 kg ha^{-1} was a non-limiting P environment to calibrate the winter dormancy rule. However, Berg et al. (2005) showed that the treatments were P limited until 2000 with the P applications resulting in significant differences in yields. Nonetheless, the winter dormancy rule achieved reasonable prediction accuracy ($R^2 = 0.71$ and CCC = 0.78) for the DM yields without the Soil-P module (*i.e.* with no P limitations) using the maximum P fertilisation rate of 75 kg ha^{-1}. This is consistent with Pembleton et al. (2011) of $R^2 = 0.53$ and CCC = 0.73 and with Ojeda et al. (2016) of $R^2 = 0.5$ and CCC = 0.77, which calibrated winter dormancy rules for alfalfa grown in Tasmania, Australia and in south-eastern Australia and the Argentine Pampas respectively. The reported RMSE of 939.54 kg ha^{-1} with an observed mean of 3529.73 kg ha^{-1} for the winter dormancy rule aligns well with findings from previous studies. For instance, Dolling et al. (2005) simulated alfalfa growth and water use across nine sites in Western Australia using ASPIM, reporting an RMSE of 1.3 Mg ha^{-1} relative to a mean observed biomass of 4.17 Mg ha^{-1}. Similarly, Chen et al. (2008) reported an RMSE of 1132 kg ha^{-1}(30 % of the mean observed biomass) for APSIM-simulated alfalfa seasonal biomass production over three growing seasons in a continuous alfalfa treatment on the Loess Plateau of Northern China. It is also important to acknowledge that the lucerne module in APSIM 7.10 is relatively less advanced than well-developed models, such as APSIM-Wheat, which may contribute to the observed model error. As the DM yields were used in our optimisation framework to enable labile P initialisation, the plant biomass P simulation performance reflects the moderate ability of APSIM to capture the P dynamics in alfalfa.

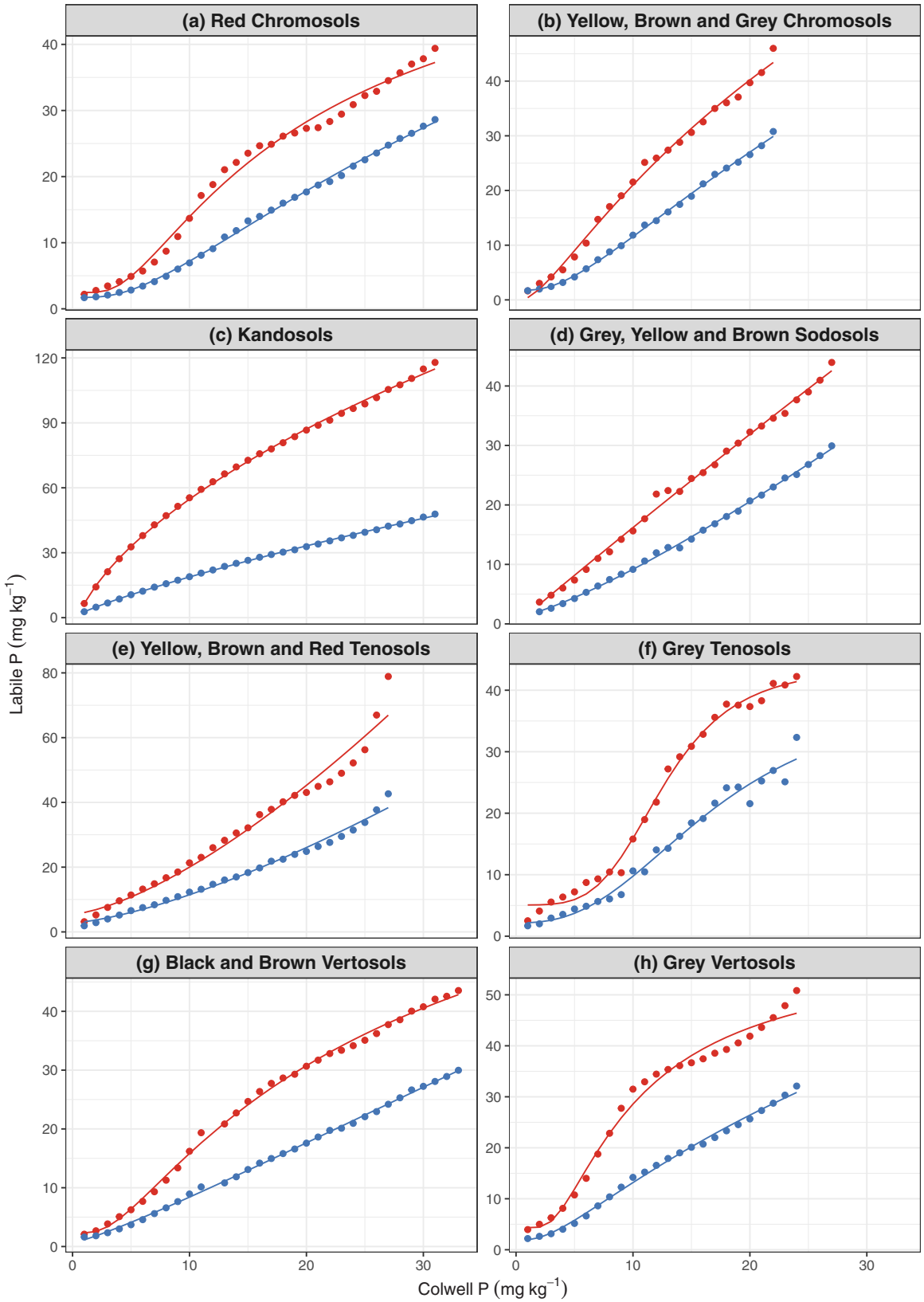

Fig. 8. Comparison of modelled labile phosphorus (P) concentrations and Colwell-extractable P (Colwell P) concentrations for the 0–10 cm soil depth interval. The dots represent discrete Colwell P values from the Colwell-P-wheat-yield response curves of Bell et al. (2013) on the x-axis and their corresponding modelled labile P values on the y-axis. The solid red line (surface layer) and the dotted navy line (subsurface layer) represent the fitted function describing the relationship between modelled labile P and Colwell P.

Table 5
Critical Colwell-extractable phosphorus (Colwell P) concentrations and its corresponding labile P concentrations for the surface and subsurface layers in APSIM at 80 %, 90 % and 95 % of maximum yield for wheat grown on soils of various Australian Soil Classification Orders and Sub-orders.

Soil Order or Suborder	Colwell P (mg kg^{-1})			Surface labile P (mg kg^{-1})			Subsurface labile P (mg kg^{-1})		
Relative Yield	80 %	90 %	95 %	80 %	90 %	95 %	80 %	90 %	95 %
(a) Red Chromosols	19	25	31	26	33	38	17	22	28
(b) Yellow, Brown and Grey Chromosols	16	20	22	33	40	44	21	27	30
(c) Kandosols	19	25	31	85	101	114	32	40	47
(d) Grey, Yellow and Brown Sodosols	17	21	25	27	33	40	17	22	26
(e) Yellow, Brown and Red Tenosols	17	21	25	39	48	58	22	28	33
(f) Grey Tenosols	16	20	23	30	38	44	19	24	28
(g) Black and Brown Vertosols	12	19	26	19	29	37	10	17	23
(h) Grey Vertosols	12	16	19	32	39	43	16	21	25

Table 6
Simulating winter dormancy for alfalfa in Indiana, United States, using manager script that controls crop responses *via* calibrated photoperiods and mean daily temperatures in APSIM.

Photoperiod (range Julian days)	Tmean (°C)	Crop class	Crop response
>199 or <85	⩽29.17	regrowth	delay
	⩽21.85	delayed	reduce
	⩽15.71	reduced	dormancy
>85 and <199	>9.6	dormant	reduce
	>10	reduced	delay
	>16	delayed	spring

This gave us confidence to apply the inverse modelling approach to APSIM to simulate crop response to different levels of labile P in a wide range of soils under diverse climates using known relationships between surface Colwell P measurements and wheat yield responses in such soils. This enabled us to determine the likely ranges of the labile P values at surface and subsurface layers in APSIM that correspond to Colwell P measurements at 0–10 cm for these soils. Soil-specific non-linear relationships between the Colwell P and surface and subsurface labile P values were then empirically derived for the major cereal cropping soils in Australia. Previous studies, such as Wang et al. (2014) and Raymond et al. (2021), have demonstrated non-linear, site-specific relationships between Colwell P and APSIM-modelled labile P for a Ferrosol and two Vertosols (The Gums and Emerald) in Queensland, Australia. Wang et al. (2014) manually calibrated initial labile P values so that simulated crop biomass and yield matched the first observed values in the no-P treatment (P_0), whereas Raymond et al. (2021) initialised the labile P pool based on the measured starting Colwell P concentrations for each soil layer. However, at the Emerald site, the initial labile P values derived directly from the measured Colwell P were insufficient to support crop growth, and a trial-and-error increase of labile P values in the surface and subsurface layers was then implemented. These studies underscored the inadequacy of directly using measured Colwell P for labile P initialisation in APSIM, given the highly non-linear relationship between these two parameters.

Our study addresses this challenge by enabling the quantitative initialisation of soil labile P based on measured soil P values for two soil series in Indiana, US, as well as for a wide range of cereal-cropping soils in Australia. We adopted P sorption levels based on the median PBCs of the surface soils in the investigated soil types, thus providing a central estimate. The derived relationships have been incorporated into an RShiny application (LinkP: https://clai317.shinyapps.io/LinkP/) to facilitate easy, quantitative initialisation of labile P in APSIM using common P test values. Users can further adjust the starting labile P values if empirical evidence suggests that their soils lie at the upper or lower ends of the reported PBC ranges. While we acknowledge that some soil types, such as Vertosols (PBC range: 5–31 mg kg^{-1} P) and Kandosols (PBC range: 4–35 mg kg^{-1} P), exhibit high variability, using the median value provides a reasonable representation for simulation purposes while minimising bias toward extreme values. We also tested simulations using the lower and upper bounds of reported PBC values (results not shown) to capture the range of variability. However, the lower-bound values for Chromosols (PBC range: 0.1–18 mg kg^{-1} P), Sodosols (0.08–8 mg kg^{-1} P), and Tenosols (1–4 mg kg^{-1} P) generally resulted in

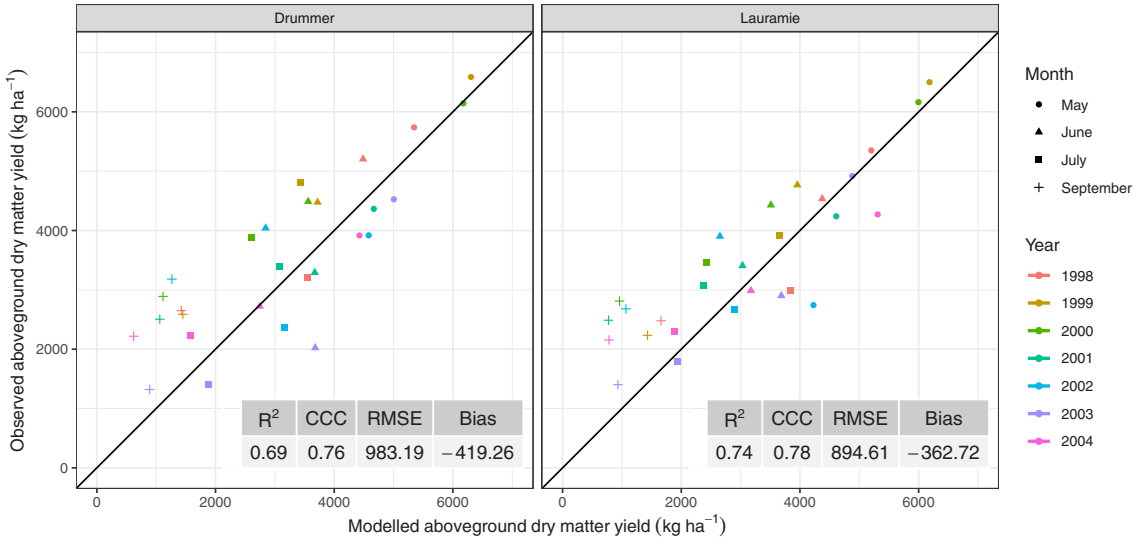

Fig. 9. Agreements of observed and modelled alfalfa aboveground dry matter yield under the optimised winter dormancy rules setting for the treatments fertilised with the maximum phosphorus fertilisation rate of 75 kg ha^{-1} by year and harvest time.

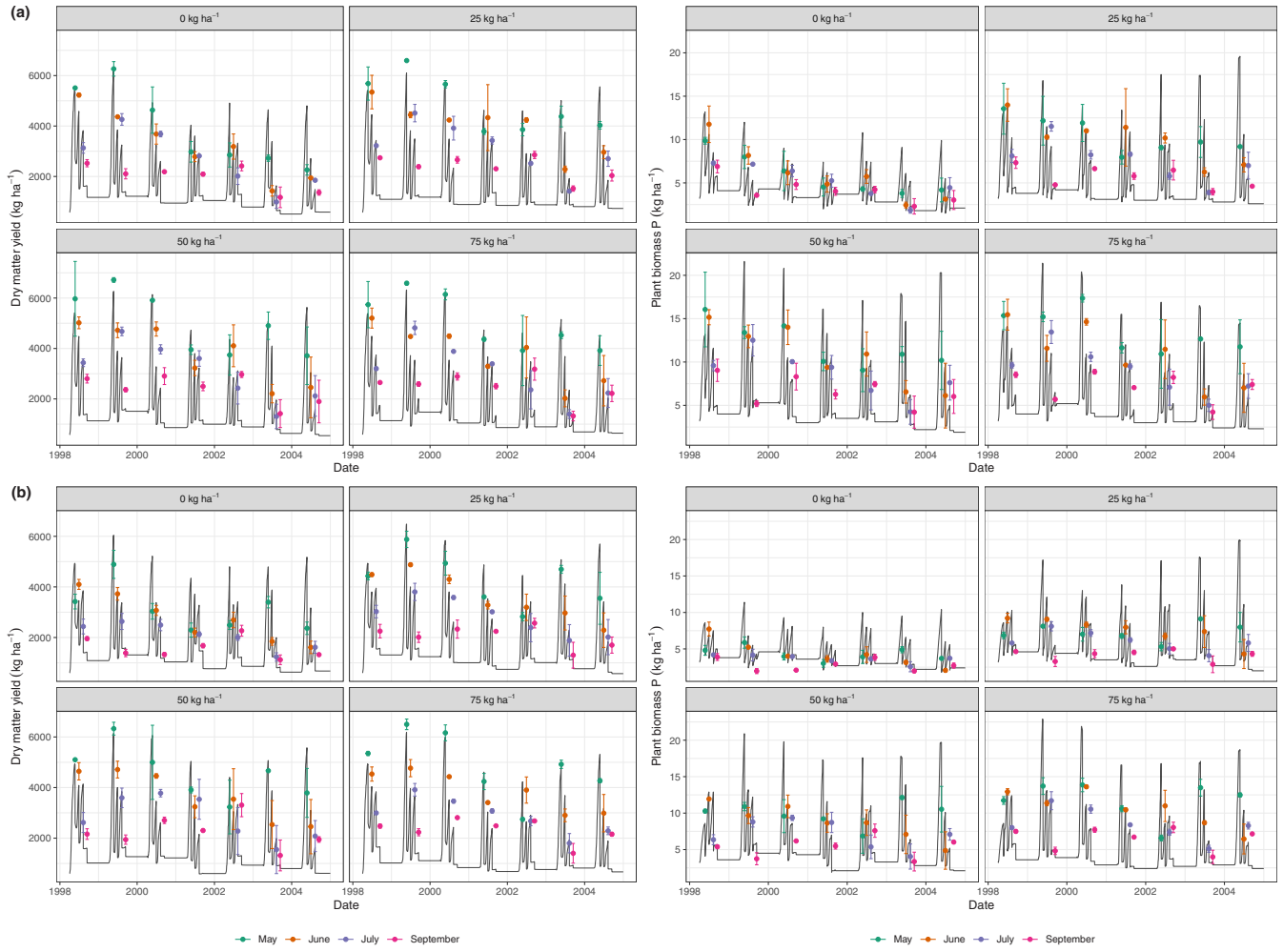

Fig. 10. Time courses of modelled (lines) and observed (dots) aboveground dry matter yields (left panel) and plant biomass phosphorus (P) contents for each of the four alfalfa harvests per year in the long-term US experiment for (a) the Drummer soil, and (b) the Lauramie soil at four different P fertiliser rates ((0, 25, 50, and 75 kg ha^{-1}). Capped vertical bars represent the standard deviation of the observed values.

failed crop simulations in APSIM at lower respective Colwell P concentrations, failing to generate labile P-yield response curves. One alternative approach might be to randomly initialise a surface sorption value within the range reported by Burkitt et al. (2002). As our study aims to facilitate the quantitative initialisation of APSIM under a wider range of conditions, this option would introduce more uncertainty in the subsequent derivation of empirical relationships. Such uncertainty could also impede the usability of derived labile P values as APSIM is unable to propagate the uncertainty of the input parameters through its modelling processes. Consequently, we opted to use median values, which provide a stable and representative baseline for our simulations while minimising variability in modelled labile P values.

Our findings demonstrate the complex relationships between measured P values and APSIM-modelled labile P values in diverse soil types and provide a quantitative approach to adjust the labile P values in APSIM to more accurately model the P dynamics across diverse agricultural soils. Different forms of sigmoidal curves, specifically Weibull functions of two different parameterisations, appeared to best represent the non-linear relationship between measured P values and APSIM-modelled labile P values. Log-logistic functions were fitted to Grey Tenosols which exhibit a symmetric sigmoidal curve with a smoother transition between the lower asymptote c to the upper asymptote d compared to the asymmetrical Weibull functions. The upper asymptote d represents the labile P initialisation value that is likely to result in maximum yield response in APSIM-Lucerne or APSIM-Wheat as Bray-2 P or Colwell P increases and might be influenced by soil buffering capacity, total phosphorus content and mineralogy. The parameter b controls the steepness of the curve, determining how quickly labile P approaches d from c so it may be related to soil sorption characteristics particularly how strongly P is fixed in the soil, while the parameter e reflects the inflection point of the curve, determining at what Bray-2 P or Colwell P x the function transitions most rapidly. Since b acts as a scaling factor on $log(x)-log(e)$, a larger e makes the function less sensitive to b. The two Weibull functions can potentially be calibrated for other soils, provided that measured P data are available.

The availability of P in soils depends on multiple factors, including soil texture, mineralogy, pH, organic matter content, and the presence of specific reactive components such as Fe and Al oxides or calcium carbonate. Clayey soils generally have higher P sorption capacity and stronger P retention compared to sandy soils due to higher surface area and cation exchange capacity (CEC) (Singh and Gilkes, 1991; Jalali and Jalali, 2016). The types of clay minerals present in a soil also heavily influence its P sorption capacity and how strongly P is retained. Smectite clays common in shrink-swell clays such as Vertisols have much higher phosphorus sorption capacities compared to non-expanding 1:1 clays such as kaolinite (Gérard, 2016). This is due to their higher CEC and greater surface area allowing more reactive sites for outer-sphere complexation and cation bridging that relatively loosely held P,

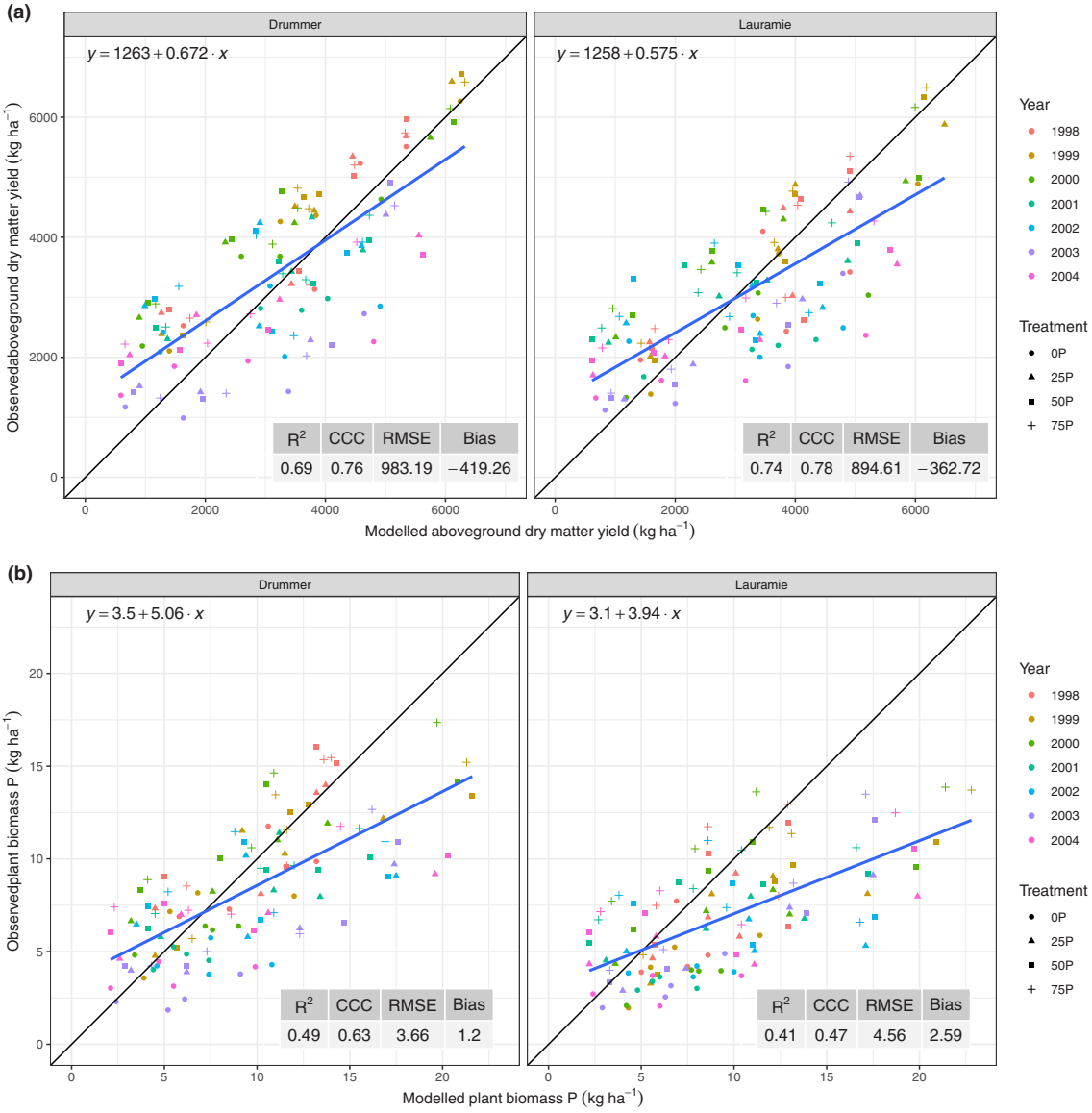

Fig. 11. Comparison of (a) observed versus modelled aboveground dry matter yields and (b) plant biomass phosphorus (P) content of alfalfa in APSIM simulations for the Drummer and Lauramie soils across four phosphorus (P) fertiliser application rates (0, 25, 50, and 75 kg ha^{-1}). The blue line represents the linear regression line fitted to the data, highlighting the relationship between observed and modelled values. Deviations of the blue line from the 1:1 line illustrate model bias: a slope < 1 indicates underprediction at higher values, a slope > 1 indicates overprediction, and an intercept $\neq 0$ reveals systematic bias.

Table 7
Statistical metrics assessing the agreement of observed and modelled alfalfa dry matter yields by year in the US experiment.

Year	R^2	CCC	RMSE (kg ha^{-1})	Bias (kg ha^{-1})
1998	0.77	0.77	678.99	−232.00
1999	0.95	0.78	818.44	−721.00
2000	0.99	0.68	1175.23	−983.75
2001	0.92	0.61	875.09	−436.12
2002	−0.12	0.13	1255.50	−350.38
2003	0.81	0.77	743.20	356.62
2004	0.93	0.65	895.07	−284.25

making them available for plant uptake. Vermiculite generally has stronger P retention compared to montmorillonite due to higher layer charge and CEC but P retained is less available to plant due to strong adsorption at interlayer sites. However, soils high in kaolinite are generally highly weathered and hence often contain high levels of Fe and Al oxides such as goethite, hematite and gibbsite, which strongly retain P making it unavailable for plant uptake. The dominant mechanism for P retention is through ligand exchange where the hydroxyl groups of Fe and Al oxides are replaced by phosphate forming strong inner-sphere complexation. This process is exacerbated under acidic conditions where kaolinite retains more P due to the protonation of surface groups promoting ligand exchange. Additionally, at low pH (<4), Al and Fe are present mostly as soluble ions, which react readily with phosphate ions to form insoluble aluminium and iron phosphates through precipitation and release H ions further acidifying the soil and reducing plant-available P. Low pH sites were excluded from the yield response curves from the BFDC database which improved their goodness of fit as low pH conditions may be associated with Al toxicity that limits root growth and hence restricts P uptake. We applied the same sorption capacity coefficient "a" for soil types within the same soil order based on Burkitt et al. (2002). However, Red Chromosols tend to have higher iron (Fe) and aluminium (Al) oxides compared to Yellow, Brown, and Grey Chromosols which could contribute to stronger P fixation and reduced P

availability. Gilkes and Hughes (1994) found that the primary determinant for P sorption in acid to neutral South-Western Australian soils is due to the amount of poorly ordered and organically complexed forms of Al which was consistent to the findings of (Singh and Gilkes, 1991). Bertrand et al. (2003) also found that amorphous Al and Fe oxides were the principal determinants of the P sorption behaviour in alkaline cropping soils of southern Australia, except in calcareous soils where the P sorption behaviour was a direction function of calcium carbonate content due to calcium phosphate precipitation making P unavailable for plants (Bertrand et al., 2003). This P adsorption decreases as soil pH increases above 8 due to decreased calcium availability (Asomaning, 2020). Soil organic matter (SOM) generally increases P retention, reduces P fixation and enhances the availability of P to plants in soils (Debicka et al., 2016; Negassa et al., 2008; Vermeiren et al., 2021). The key mechanisms by which SOM influences P sorption and availability in soils include: 1. competitive adsorption of SOM with P for binding sites; 2. metal complexation and dissolution reactions reducing available adsorption sites; 3. increased repulsion of phosphate anions by sorption of OM to positive sorption sites; and 4. formation of cation bridging particularly between P and humic and fulvic acids leading to increased sorption (Guppy et al., 2005; Hunt et al., 2007).

This study focused primarily on the relationship between labile P values and the sorption capacity coefficients while maintaining default values for other key input parameters in APSIM such as the root C:P ratio, the rate of dissolution of rock P, the sorption coefficient *b*, and the rate loss available (*r* coefficient). This conservative approach helps reduce potential noise in model outputs. Since the rock phosphate content was initialised to zero in our simulations, the rate of rock P dissolution parameter did not affect our reported outcomes here. However, in experiment-based studies where rock phosphate is present, this parameter could play a significant role in determining phosphorus availability and overall model performance. Therefore, when applying the model to soils with substantial rock phosphate reserves, careful calibration of the rate of rock P dissolution is recommended to accurately capture its impact on soil P dynamics. Raymond et al. (2021) showed that the optimal *r* values that produced relative increases in APSIM-modelled labile P comparable to measured changes in Colwell P appeared to be both site- and P-fertilisation rate-specific, suggesting that the *r* coefficient might be influenced by "as-yet-unidentified" soil characteristics. These characteristics might include soil microbial diversity and activity such as phosphate solubilising bacteria and mycorrhizal fungi that significantly affect P transformations between organic, inorganic and residual pools (Zhang et al., 2021) which are not yet captured by the model. Users are therefore encouraged to perform sensitivity analyses on these additional parameters and to adjust them only when modelling specific experimental conditions for which sufficient empirical data are available.

Currently, only limited crops have been parameterised for P use in APSIM and only in limited environments. Future research should also aim to incorporate current understanding of differences in P use efficiencies of different crop types in agricultural systems models to improve our ability to use these models for deriving practical solutions. The Colwell P-relative yield response curves from the BFDC database used provided generalised information on crop yield responses to surface P soil test measurements of different soils. The present study helps to extend the information from the BFDC database to agricultural cropping systems modelling to enable the incorporation of climate and management considerations in P fertiliser decision-making. Bell et al. (2013) stated that overall crop yields increased over time, likely due to advancements in crop varieties and agronomic management. These improvements may have introduced variability in yield response curves, leading to differences in their goodness of fit (*r*). The present study focused on the more robust wheat yield response curves of P from the BFDC database as the wheat experiments were most extensive. This could serve as a starting point to better define soil P requirements for other crops known to have different P use efficiencies by extending the information on such crops from the BFDC database to soil and crop parameterisation in APSIM using the present study as a benchmark. Bell et al. (2013) noted that they used $r \geq 0.4$ as a minimum threshold for establishing critical Colwell P values. All soil types included in our study have *r* above 0.45. We also conducted all simulations using the check variety Hartog with a consistent management regime across the study period. This minimises the confounding effects of agronomic advancements. Nonetheless, we acknowledge that this uncertainty was not propagated in our modelling. The current implementation of crop P responses in APSIM 7.10 is not variety specific. Future studies could extend the current model framework by integrating varietal and management dynamics, potentially through a sensitivity analysis or the development of variety-specific response functions in APSIM.

Future research might consider incorporating the derived relationships in farmer-oriented decision support tools such as ARMOnline (Phelan et al., 2018; Quigley et al., 2019) or NrX(https://www.regrow.ag/case-studies/agretail) and the application of the inverse modelling approach at agricultural locations represented in such tools to improve the location specificity of the relationships and enable the development of more accurate and practical soil P management recommendations. This will depend upon the availability of P measurements correlated with yields of different crops. The accuracy of the relationships between measured soil test values and labile P conditions in APSIM can be further improved when the P sorption capacities of the soils are measured. Combining measurement and modelling thus bridges the gap in assessing P dynamics in complex soil-plant-climate-management systems and will enhance our ability to inform P management to improve P use efficiencies.

5. Conclusions

Our results showed that APSIM adequately represents P dynamics in alfalfa and wheat crops under different environment (climate × soil) × management combinations. We derived empirical relationships between soil test P values and the labile P pool in APSIM for a wide range of soils using an inverse modelling approach. These relationships differ for different soil types, emphasising the significance of accurate characterisation of soil P sorption capacities and the availability of P measurements correlated with yields of different crops. The derived empirical relationships will facilitate the quantitative initialisation of conceptual labile P pools and calibration of P parameters using common P test values in agricultural systems models such as APSIM. This thus addresses a key challenge in the practical application of such models to inform P fertilisation management and to improve the use efficiency of this macro-nutrient. Future research should aim to extend the information on P use efficiencies of other crops and to explore more advanced optimisation techniques to further improve the accuracy of our estimates.

CRediT authorship contribution statement

Yunru Lai: Writing – original draft, Visualization, Methodology, Investigation, Formal analysis, Data curation, Conceptualization. **Jonathan J Ojeda:** Writing – review & editing, Methodology, Data curation. **Simon Clarendon:** Writing – review & editing. **Nathan Robinson:** Writing – review & editing. **Enli Wang:** Writing – review & editing. **Keith Pembleton:** Writing – review & editing, Methodology.

Declaration of Competing Interest

The authors declare that they have no known competing financial interests or personal relationships that could have appeared to influence the work reported in this paper.

Data availability

Data will be made available on request.

Acknowledgements

This work has been supported by the Cooperative Research Centre for High Performance Soils (Grant Number 4.3.002) whose activities are funded by the Australian Government's Cooperative Research Centre Program. We also acknowledge the support of the University of Southern Queensland for providing access to the Fawkes high-performance computing cluster used in this research. Acknowledgement is made to the APSIM Initiative which takes responsibility for quality assurance and a structured innovation program for APSIM's modelling software, which is provided free for research and development use (see www.apsim.info for details). We are also grateful for the insightful comments made by Dr. Lukas van Zwieten of the New South Wales Department of Primary Industries in response to the draft of this paper.

Appendix A. Supporting information

Supplementary data associated with this article can be found in the online version at doi:10.1016/j.still.2025.106532.

References

Ahmed, M., Ijaz, W., Ahmad, S., 2018. Adapting and evaluating apsim-soilp-wheat model for response to phosphorus under rainfed conditions of pakistan. J. Plant Nutr. 41, 2069–2084. https://doi.org/10.1080/01904167.2018.1485933.

Asomaning, S., 2020. Processes and factors affecting phosphorus sorption in soils. In: Kyzas, G.Z., Lazaridis, N.A. (Eds.), Sorption in 2020s. IntechOpen. chapter 3, pp. 1–16 https://www.intechopen.com/chapters/90719, 10.5772/intechopen.90719.

Bell, R., Reuter, D., Scott, B., Sparrow, L., Strong, W., the late Chen, W., 2013. Soil phosphorus–crop response calibration relationships and criteria for winter cereal crops grown in Australia. Crop Pasture Sci. 64, 480–498. https://doi.org/10.1071/cp13016.

Berg, W., Cunningham, S., Brouder, S., Joern, B., Johnson, K., Santini, J., Volenec, J., 2005. Influence of phosphorus and potassium on alfalfa yield and yield components. Crop Sci. 45, 297–304. https://doi.org/10.2135/cropsci2005.0297.

Berg, W.K., Cunningham, S.M., Brouder, S.M., Joern, B.C., Johnson, K.D., Santini, J.B., Volenec, J.J., 2007. The long-term impact of phosphorus and potassium fertilization on alfalfa yield and yield components. Crop Sci. 47, 2198–2209. https://doi.org/10.2135/cropsci2006.09.0576.

Berg, W.K., Cunningham, S.M., Brouder, S.M., Joern, B.C., Johnson, K.D., Volenec, J.J., 2009. Influence of phosphorus and potassium on alfalfa yield, taproot C and N pools, and transcript levels of key genes after defoliation. Crop Sci. 49, 974–982. https://doi.org/10.2135/cropsci2008.07.0395.

Berg, W.K., Lissbrant, S., Volenec, J.J., Brouder, S.M., Joern, B.C., Johnson, K.D., Cunningham, S.M., 2020.Phosphorus and Potassium Influence on Alfalfa Nutrition (Version 2.0).⟨https://purr.purdue.edu/publications/1004/2⟩, 10.4231/PPKB-VK18.

Bertrand, I., Holloway, R., Armstrong, R., Mclaughlin, M., 2003. Chemical characteristics of phosphorus in alkaline soils from southern Australia. Soil Res. 41, 61–76. https://doi.org/10.1071/SR02021.

Bishop, T.F.A., McBratney, A.B., Laslett, G.M., 1999. Modelling soil attribute depth functions with equal-area quadratic smoothing splines. Geoderma 91, 27–45. https://doi.org/10.1016/s0016-7061(99)00003-8.

Brown, H.E., Huth, N.I., Holzworth, D.P., Teixeira, E.I., Zyskowski, R.F., Hargreaves, J.N.G., Moot, D.J., 2014. Plant modelling framework: software for building and running crop models on the APSIM platform. Environ. Model. Softw. 62, 385–398. https://doi.org/10.1016/j.envsoft.2014.09.005.

Burkitt, L.L., Moody, P.W., Gourley, C.J.P., Hannah, M.C., 2002. A simple phosphorus buffering index for Australian soils. Soil Res. 40, 497–513. https://doi.org/10.1071/sr01050.

Cakmak, I., 2002. Plant nutrition research: priorities to meet human needs for food in sustainable ways. Plant Soil 247, 3–24.

Carpenter, S.R., Caraco, N.F., Correll, D.L., Howarth, R.W., Sharpley, A.N., Smith, V.H., 1998. Nonpoint pollution of surface waters with phosphorus and nitrogen. Ecol. Appl. 8, 559–568. https://doi.org/10.1890/1051-0761(1998)008[0559:nposww]2.0.co;2.

Chapagain, R., Remenyi, T.A., Harris, R.M., Mohammed, C.L., Huth, N., Wallach, D., Rezaei, E.E., Ojeda, J.J., 2022. Decomposing crop model uncertainty: a systematic review. Field Crops Res. 279, 108448. https://doi.org/10.1016/j.fcr.2022.108448.

Chen, W., Shen, Y., Robertson, M., Probert, M., Bellotti, W., 2008. Simulation analysis of lucerne-wheat crop rotation on the loess plateau of northern china. Field Crops Res. 108, 179–187. https://doi.org/10.1016/J.FCR.2008.04.010.

Childers, D.L., Corman, J., Edwards, M., Elser, J.J., 2011. Sustainability challenges of phosphorus and food: solutions from closing the human phosphorus cycle. Bioscience 61, 117–124. https://doi.org/10.1525/bio.2011.61.2.6.

Cordell, D., White, S., 2014. Life's bottleneck: sustaining the world's phosphorus for a food secure future. Annu. Rev. Environ. Resour. 39, 161–188. https://doi.org/10.1146/annurev-environ-010213-113300.

Dalgliesh, N., Cocks, B., Horan, H., 2012.APSoil-providing soils information to consultants, farmers and researchers, In: 16th Australian Agronomy Conference, Armidale, NSW.⟨https://www.agronomyaustraliaproceedings.org/images/sampledata/2012/7993_5_dalgliesh.pdf⟩.

Das, B., Huth, N., Probert, M., Condron, L., Schmidt, S., 2019. Soil phosphorus modeling for modern agriculture requires balance of science and practicality: a perspective. J. Environ. Qual. 48, 1281–1294. https://doi.org/10.2134/jeq2019.05.0201.

Debicka, M., Kocowicz, A., Weber, J., Jamroz, E., 2016. Organic matter effects on phosphorus sorption in sandy soils. Arch. Agron. Soil Sci. 62, 840–855. https://doi.org/10.1080/03650340.2015.1083981.

Delve, R.J., Probert, M.E., Cobo, J.G., Ricaurte, J., Rivera, M., Barrios, E., Rao, I.M., 2009. Simulating phosphorus responses in annual crops using APSIM: model evaluation on contrasting soil types. Nutr. Cycl. Agroecosystems 84, 293–306. https://doi.org/10.1007/s10705-008-9243-6.

Denning, J., Eliason, R., Goos, R., Hoskins, B., Nathan, M., Wolf, A., 1998.Recommended chemical soil test procedures for the north central region. North Central Regional Research Publication 221.

Dokoohaki, H., Miguez, F.E., Archontoulis, S., Laird, D., 2018. Use of inverse modelling and bayesian optimization for investigating the effect of biochar on soil hydrological properties. Agric. Water Manag. 208, 268–274. https://doi.org/10.1016/j.agwat.2018.06.034.

Dolling, P., Robertson, M., Asseng, S., Ward, P., Latta, R., 2005. Simulating lucerne growth and water use on diverse soil types in a mediterranean-type environment. Crop Pasture Sci. 56, 503–515. https://doi.org/10.1071/AR04216.

Fosu-Mensah, B.Y., MacCarthy, D.S., Vlek, P.L.G., Safo, E.Y., 2012. Simulating impact of seasonal climatic variation on the response of maize (*Zea mays* L.) to inorganic fertilizer in sub-humid Ghana. Nutr. Cycl. Agroecosystems 94, 255–271. https://doi.org/10.1007/s10705-012-9539-4.

Gao, F., Han, L., 2012. Implementing the nelder-mead simplex algorithm with adaptive parameters. Comput. Optim. Appl. 51, 259–277. https://doi.org/10.1007/s10589-010-9329-3.

Gérard, F., 2016. Clay minerals, iron/aluminum oxides, and their contribution to phosphate sorption in soils—a myth revisited. Geoderma 262, 213–226. https://doi.org/10.1016/j.geoderma.2015.08.036.

Gilkes, R., Hughes, J., 1994. Sodium-fluoride ph of south-western australian soils as an indicator of p-sorption. Soil Res. 32, 755–766. https://doi.org/10.1071/SR9940755.

Guppy, C.N., Menzies, N., Moody, P.W., Blamey, F., 2005. Competitive sorption reactions between phosphorus and organic matter in soil: a review. Soil Res. 43, 189–202. https://doi.org/10.1071/sr04049.

He, S., Long, M., He, X., Guo, L., Yang, J., Yang, P., Hu, T., 2017. Arbuscular mycorrhizal fungi and water availability affect biomass and c: N: P ecological stoichiometry in alfalfa (Medicago sativa l.) during regrowth. Acta Physiol. Plant. 39, 1–9. https://doi.org/10.1007/s11738-017-2493-7.

Holzworth, D.P., Huth, N.I., deVoil, P.G., Zurcher, E.J., Herrmann, N.I., McLean, G., Chenu, K., van Oosterom, E.J., Snow, V., Murphy, C., et al., 2014. Apsim–evolution towards a new generation of agricultural systems simulation. Environ. Model. Softw. 62, 327–350. https://doi.org/10.1016/j.envsoft.2014.07.009.

Hunt, J., Ohno, T., He, Z., Honeycutt, C., Dail, D.B., 2007. Inhibition of phosphorus sorption to goethite, gibbsite, and kaolin by fresh and decomposed organic matter. Biol. Fertil. Soils 44, 277–288. https://doi.org/10.1007/s00374-007-0202-1.

Isbell, R., 2021. The national committee on soil and terrain. The Australian Soil Classification, Third ed. CSIRO Publishing, Melbourne, Victoria, Australia. https://doi.org/10.1071/9781486314782.

Jalali, M., Jalali, M., 2016. Relation between various soil phosphorus extraction methods and sorption parameters in calcareous soils with different texture. Sci. Total Environ. 566, 1080–1093. https://doi.org/10.1016/j.scitotenv.2016.05.133.

Jeffrey, S.J., Carter, J.O., Moodie, K.B., Beswick, A.R., 2001. Using spatial interpolation to construct a comprehensive archive of australian climate data. Environ. Model. Softw. 16, 309–330.

Jiménez, J.G., Healy, M., Daly, K., 2019. Effects of fertiliser on phosphorus pools in soils with contrasting organic matter content: a fractionation and path analysis study. Geoderma 338, 128–135. https://doi.org/10.1016/j.geoderma.2018.11.049.

Keating, B.A., Carberry, P.S., Hammer, G.L., Probert, M.E., Robertson, M.J., Holzworth, D., Huth, N.I., Hargreaves, J.N.G., Meinke, H., Hochman, Z., et al., 2003. An overview of APSIM, a model designed for farming systems simulation. Eur. J. Agron. 18, 267–288. https://doi.org/10.1016/s1161-0301(02)00108-9.

Lin, L.I.K., 1989. A concordance correlation coefficient to evaluate reproducibility. Biometrics 45, 255–268. https://doi.org/10.2307/2532051. ⟨https://www.jstor.org/stable/2532051⟩.

Lissbrant, S., Stratton, S., Cunningham, S., Brouder, S., Volenec, J., 2009. Impact of long-term phosphorus and potassium fertilization on alfalfa nutritive value–yield relationships. Crop Sci. 49, 1116–1124. https://doi.org/10.2135/cropsci2008.06.0333.

Lu, J., He, S., Wang, Z., Yang, H., 2016. Carbon, nitrogen and phosphorus stoichiometry in differently aged lucerne stands during flowering. Legume Res. Int. J. 39, 595–600. https://doi.org/10.18805/lr.v0iof.9612.

Lu, J., Liu, M., Yang, M., Xie, J., Yang, H., Li, L., 2020. Leaf resorption and stoichiometry of n and p of 1, 2 and 3 year-old lucerne under one-time p fertilization. Soil Tillage Res. 197, 104481. https://doi.org/10.1016/j.still.2019.104481.

Lu, J., Yang, M., Liu, M., Wang, Y., Yang, H., 2019. Leaf stoichiometry and resorption of n and p in lucerne at different growth stages under different water supplies. J. Plant Nutr. 42, 501–511. https://doi.org/10.1080/01904167.2019.1567776.

Meier, E.A., Hunt, J.R., Hochman, Z., 2021. Evaluation of nitrogen bank, a soil nitrogen management strategy for sustainably closing wheat yield gaps. Field Crops Res. 261, 108017. https://doi.org/10.1016/j.fcr.2020.108017.

Metson, G.S., Iwaniec, D.M., Baker, L.A., Bennett, E.M., Childers, D.L., Cordell, D., Grimm, N.B., Grove, J.M., Nidzgorski, D.A., White, S., 2015. Urban phosphorus sustainability: systemically incorporating social, ecological, and technological factors into phosphorus flow analysis. Environ. Sci. Policy 47, 1–11. https://doi.org/10.1016/j.envsci.2014.10.005.

Micheni, A.N., Kihanda, F.M., Warren, G.P., Probert, M.E., 2004.Testing the APSIM model with experimental data from the long-term manure experiment at Machang'a (Embu), Kenya, In: ACIAR PROCEEDINGS, ACIAR; 1998.110-117.

Negassa, W., Dultz, S., Schlichting, A., Leinweber, P., 2008. Influence of specific organic compounds on phosphorus sorption and distribution in a tropical soil. Soil Sci. 173, 587–601. https://doi.org/10.1097/SS.0b013e3181847eef.

Ojeda, J.J., Pembleton, K.G., Islam, M.R., Agnusdei, M.G., Garcia, S.C., 2016. Evaluation of the agricultural production systems simulator simulating lucerne and annual ryegrass dry matter yield in the argentine pampas and south-eastern australia. Agric. Syst. 143, 61–75.

Ojeda, J.J., Volenec, J.J., Brouder, S.M., Caviglia, O.P., Agnusdei, M.G., 2017. Evaluation of Agricultural Production Systems Simulator as yield predictor of Panicum virgatum and Miscanthus x giganteus in several US environments. GCB Bioenergy 9, 796–816.

Pembleton, K.G., Rawnsley, R.P., Donaghy, D.J., 2011. Yield and water-use efficiency of contrasting lucerne genotypes grown in a cool temperate environment. Crop Pasture Sci. 62, 610–623. https://doi.org/10.1071/cp11094.

Pembleton, K.G., Sathish, P., 2014. Giving drought the cold shoulder: a relationship between drought tolerance and fall dormancy in an agriculturally important crop. AoB Plants 6, plu012. https://doi.org/10.1093/aobpla/plu012.

Phelan, D.C., Harrison, M.T., McLean, G., Cox, H., Pembleton, K.G., Dean, G.J., Parsons, D., do Amaral Richter, M.E., Pengilley, G., Hinton, S.J., et al., 2018. Advancing a farmer decision support tool for agronomic decisions on rainfed and irrigated wheat cropping in tasmania. Agric. Syst. 167, 113–124. https://doi.org/10.1016/j.agsy.2018.09.003.

Probert, M.E., 1985. A conceptual model for initial and residual responses to phosphorus fertilizers. Fertil. Res. 6, 131–138. https://doi.org/10.1007/bf01051007.

Probert, M.E., 2004.A capability in APSIM to model phosphorus responses in crops, In: ACIAR PROCEEDINGS, Citeseer.92-100.

Quigley, M.C., Bennetts, L.G., Durance, P., Kuhnert, P.M., Lindsay, M.D., Pembleton, K. G., Roberts, M.E., White, C.J., 2019. The provision and utility of science and uncertainty to decision-makers: earth science case studies. Environ. Syst. Decis. 39, 307–348. https://doi.org/10.1007/s10669-019-09728-0.

Raymond, N., Kopittke, P.M., Wang, E., Lester, D., Bell, M.J., 2021. Does the APSIM model capture soil phosphorus dynamics? a case study with Vertisols. Field Crops Res. 273, 108302. https://doi.org/10.1016/j.fcr.2021.108302.

Robertson, M., Carberry, P., Huth, N., Turpin, J., Probert, M.E., Poulton, P., Bell, M., Wright, G., Yeates, S., Brinsmead, R., 2002. Simulation of growth and development of diverse legume species in apsim. Aust. J. Agric. Res. 53, 429–446. https://doi.org/10.1071/ar01106.

Sakamoto, Y., Ishiguro, M., Kitagawa, G., 1986. Akaike information criterion statistics. Dordrecht, The Netherlands: D. Reidel 81, 26853.10.2307/2348776.

Seber, G.A.F., Wild, C.J., 1989. Growth models. John Wiley & Sons, New York, pp. 338–339. https://doi.org/10.1002/0471725315.

Singer, S., Nelder, J., 2009. Nelder-mead algorithm. Scholarpedia 4, 2928. https://doi.org/10.4249/scholarpedia.2928.

Singh, B., Gilkes, R., 1991. Phosphorus sorption in relation to soil properties for the major soil types of south-western australia. Soil Res. 29, 603–618. https://doi.org/10.1071/SR9910603.

Tedeschi, L.O., 2006. Assessment of the adequacy of mathematical models. Agric. Syst. 89, 225–247. https://doi.org/10.1016/j.agsy.2005.11.004.

Vermeiren, C., Kerckhof, P., Reheul, D., Smolders, E., 2021. Increasing soil organic carbon content can enhance the long-term availability of phosphorus in agricultural soils. Eur. J. Soil Sci. 73. https://doi.org/10.1111/ejss.13191.

Wang, E., Bell, M., Luo, Z., Moody, P., Probert, M.E., 2014. Modelling crop response to phosphorus inputs and phosphorus use efficiency in a crop rotation. Field Crops Res. 155, 120–132. https://doi.org/10.1016/j.fcr.2013.09.015.

Woodson, P., Volenec, J.J., Brouder, S.M., 2013. Field-scale potassium and phosphorus fluxes in the bioenergy crop switchgrass: theoretical energy yields and management implications. J. Plant Nutr. Soil Sci. 176, 387–399. https://doi.org/10.1002/jpln.201200294.

Zhang, Y., Finn, D., Bhattacharyya, R., Dennis, P., Doolette, A., Smernik, R., Dalal, R., Meyer, G., Lombi, E., Klysubun, W., Jones, A., Wang, P., Menzies, N., Kopittke, P., 2021.Long-term changes in land use influence phosphorus concentrations, speciation, and cycling within subtropical soils.Geoderma 10.1016/J.GEODERMA.2021.115010.